

# Methodological challenges of scenario generation validation: a rear-end crash-causation model for virtual safety assessment

Jonas Bärgrman<sup>1)</sup>, Malin Svärd<sup>2)</sup>, Simon Lundell<sup>2)</sup> and Erik Hartelius<sup>2)</sup>

1) Division of Vehicle Safety, Department of Applied Mechanics, Chalmers University of Technology

2) Volvo Car Corporation, Volvo Cars Safety Centre

## Abstract

Vehicle conflict and crash avoidance systems are becoming increasingly common on our roads, aiming to save lives and mitigate injuries. System developers and other stakeholders need methods to assess the safety benefit of these systems before they are introduced. Using computer simulations for this is increasingly common, and a core component is the generation of crashes virtually. Crashes can be generated in several ways; one is to use models of crash causation, applied to pre-crash kinematics from in-depth crash databases. However, these models are seldomly thoroughly validated. To address this research gap this study aims to validate a rear-end crash-causation-theory model based on four crash-causation mechanisms: a) off-road glances, b) driving with too short headway, c) drivers not braking with the maximum deceleration possible, and d) sleepy drivers (no reaction before the crash). Pre-crash kinematics from the German GIDAS in-depth crash database were used as a basis for validation. For each original crash, the evasive maneuver of the following vehicle was replaced with the crash-causation model. Comparisons were then made between the estimated delta-v distribution of the original GIDAS data and the delta-v distribution of the generated crashes. During the work, challenges with the validation process were identified and addressed; most notably a process for transforming the generated crashes (which intrinsically include a large proportion of property-damage-only crashes) was developed, to mimic the sample selection process of GIDAS, addressing the GIDAS selection bias related to censoring of low-severity crashes. Our results indicate that a sample selection bias transform is likely to substantially improve the comparability (and thus validation accuracy) of scenarios generated with a crash-causation model and GIDAS data. Our results further show that the proposed crash-causation model is a reasonably good crash generator, although the delta-v distribution is somewhat shifted towards lower values compared to the GIDAS distribution.

This work highlights the need for a thorough understanding of both the scenario generation process and the validation dataset when aiming to validate the outcome of scenario generation through virtual simulation. Much more work on the development of validation processes for scenario generation is needed, across all levels of crash severity.

**Keywords:** crash-causation; scenario generation; validation; driver model; safety assessment; counterfactual simulations

## 1 Introduction

Automotive systems that aim to improve road safety by avoiding conflicts and crashes have undergone massive improvements in the last 20 years. These systems include different levels of vehicle automation, such as Advanced Driver Assistance Systems (ADASs) and Automated Driving Systems (ADSs). ADASs have primarily included crash avoidance systems such as Automated Emergency Braking (AEB; Benmimoun, Pütz, Zlocki, & Eckstein, 2013), which brake automatically when a crash is imminent. Conflict avoidance systems such as Adaptive Cruise Control (ACC), which maintain the distance to a lead vehicle, are now routinely included as well. In contrast, ADSs go beyond just providing support, taking on the entire driving task (at least under some conditions; Bjorvatn et al., 2021). Consequently, while ADS' primary focus is on conflict avoidance in everyday driving, crash avoidance systems such as AEB are also present, ready to act if a conflict cannot be avoided.

It is important that developers of conflict and crash avoidance systems, as well as other stakeholders such as governments and consumer rating organizations (e.g., NCAP; Miller et al., 2014), have the tools to efficiently and reliably assess the systems' safety impact. There are many ways to do so, but when the assessment needs to be done during the system's development or soon after its deployment, the number of methods available are limited because of the lack of real-world data. One method that has been receiving great attention recently is the use of virtual simulation to compare 'baseline' traffic situations (without the system) with 'treatment' traffic situations (with the system virtually applied). The comparison typically entails assessing the proportion of baseline crashes that are completely avoided in the treatment simulations, but the mean of the impact speeds or injury risk (or some metric describing their entire distributions) for the baseline and treatment simulations can also be compared.

A core component of the virtual-simulation method is an accurate, realistic baseline—the set of conflict situations to which the system under assessment is applied for comparison. There are several different ways to create a baseline for a specific assessment. One way is to directly use digital representations of actual (reconstructed) crashes (Schubert, 2013). Another is to create them synthetically (Wimmer, 2023).

There are several reasons why synthetic baseline generation is more enticing than using actual crash data. Firstly, crashes are rare, which means that the statistical power of an assessment that only uses actual crashes is often limited. Secondly, collecting data from actual crashes is very costly. Creating synthetic crashes in a virtual environment is likely to be substantially cheaper. Thirdly, crash data represent the crashes of "yesterday"; they are not necessarily representative of the crashes of today or the future—especially with the introduction of ADS. If synthetically generated crashes can truly represent a real-world crash distribution, then they can ensure the validity of safety system assessments and improve the (virtual) prospective assessments of safety technologies in traffic environments of the future.

There are different ways to generate synthetic baselines: a) without simulation, by sampling from a multi-dimensional joint distribution space which describes the pre-crash kinematics in detail, either as variations of actual crashes (Leledakis et al., 2021) or of crashes created synthetically from distributions (Wimmer, 2023); b) through virtual simulations of traffic interactions based on models of road user interactions, where the initial conditions are based on distributions (Fries, Fahrenkrog, Donauer, Mai, & Raisch, 2022; Helmer, Wang, Kompass, & Kates, 2015; van Lint & Calvert, 2018); and c) through virtual simulations that generate variations of actual conflicts, by keeping some of the actual conflict kinematics while replacing others with driver behavior models (Bärgman, Lisovskaja, Victor, Flannagan, & Dozza, 2015; Bärgman & Victor, 2019; Lee, Lee, Bärgman, Lee, & Reimer, 2018).

Whichever method is used to create synthetic crashes, the outcome should be a reasonable representation of the real-world scenario they seek to represent. If the baseline does not represent the real-world the impact assessment will likely not be accurate. The measures of interest—such as, for rear-end crashes, the distribution of impact speeds or the change in speed during the crash (delta-v) of the generated crashes—should be reasonably similar for the synthetically generated baseline crashes and the actual crashes they represent. This work set out to validate a method, based on crash-causation theory, aimed to generate realistic baseline scenarios for rear-end crashes.

The theory-based crash-causation model (hereafter called the TBM for convenience) consists of four sub-models, each named after the rear-end crash-causation mechanism that it describes: 1) Off-road glances (when off-road glances delay the braking response), 2) Too-close (when drivers are driving too close to the lead vehicle), 3) Low-deceleration (when drivers do not brake as hard as the car and the environment permit), and 4) No-response (when drivers are sleepy or drowsy).

As for the first mechanism, several studies have shown off-road glances to be a main contributing factor to crashes (Hickman, Hanowski, & Bocanegra, 2010; Klauer et al., 2014; Victor et al., 2015), especially in rear-end crashes. In fact, glances off-road have been shown to substantially increase crash and injury risks in manual driving (Klauer et al., 2014; Victor et al., 2015). However, many drivers follow a lead vehicle too closely, so crashes can occur even when drivers have their eyes on the forward roadway. This situation is described by Too-close, the second crash-causation mechanism.

Further, when drivers are about to crash, they often do not brake as hard as possible, in terms of what the car is capable of and what the environment (such as road surface) would support (Low-deceleration, the third crash-causation mechanism; (Bärgman, Boda, & Dozza, 2017; Fajen, 2005; Kusano & Gabler, 2012). That is, they might have been able to avoid the crash, or at least lower the crash speed, if they had braked harder. This crash-causation mechanism is 'independent of' and 'in addition to' the first two mechanisms.

Finally, the fourth crash-causation mechanism described in one of the sub-models is No-response drivers. While Knipling and Wang (1994) estimate that the proportion of rear-end crash cases caused by sleepy drivers is 6.6%, others have estimated the proportion to be between 9% and 20% (Horne & Reyner, 1999). The No-response mechanism includes all following-vehicle drivers who are fatigued or sleepy, and therefore completely fail to brake in response to the evolving conflict with the lead vehicle, causing a crash at maximum impact speed (i.e., there is no reduction in speed of the following vehicle during the event).

Together, these four crash-causation mechanisms are included in the TBM model to be validated in this work because they account for a large proportion of rear-end crashes on our roads (Horne & Reyner, 1999; Kiefer, Salinger, & Ference, 2005; Klauer et al., 2014). However, the fact that the proportion of crashes caused by each individual crash-causation mechanism is not known with certainty may impact the validity of theory-based, baseline-scenario generation models, such as the TBM in this study.

With respect to the validation process of synthetically generated baselines, it is not obvious what to validate against. Optimally, data from real-world crash databases that include **all** levels of severity should be used (unfortunately, such data are typically not available). While crashes generated through simulation typically include all levels of severity (even the lowest-severity, property-damage-only (PDO) crashes), real-world databases do not. Specifically, if validation is to be performed comparing the outcome of synthetically generated baseline crashes with crashes from a crash database with a selection bias (in practice, all currently available crash databases), that bias must be considered in order for the comparison to be meaningful. Basically, all crash databases censor lower-severity crashes for failing to meet some inclusion criteria. For example, they might only include crashes when someone is injured (e.g., German In Depth Accident Study; GIDAS; Schubert, 2013), when repair costs are greater than a given threshold (Isaksson-Hellman & Norin, 2005; Ydenius, Stigson, Kullgren, & Sunnevang, 2013), or when a vehicle has to be towed from the scene (US-DOT, 1998). In any case, censored crashes will not be in the database. One may argue that the application of injury risk curves mitigates the bias effect, but we found no studies quantifying to what extent the bias is mitigated if this is done. Also, the authors of the current paper have not found any literature that specifically investigates other methods of mitigating the selection bias to enable accurate validation of the baseline generation.

Fortunately, when it comes to quantifying the selection bias itself, studies have estimated the proportion of PDO crashes in crashes of all severity levels (of a specific scenario type). The proportion is typically large. For example, Knipling et al. (1992) estimated that approximately 70-75% of all rear-end crashes are PDO crashes (see Appendix A for details).

There are, however, databases that include some PDO crashes, such as the Folksam insurance company's database (Ydenius et al., 2013). For inclusion in their database, the crashes must incur repair costs above a certain threshold; less costly PDO crashes are missing. Since there are estimates of the overall proportion of PDO crashes (at least for some scenarios), it should

be possible to complement the PDO crashes that are available (e.g., in the Folksam database) with estimates of the ones that are missing.

## **1.4 Objectives**

This work set out to validate a model that generates baseline rear-end crash scenarios using four known crash-causation mechanisms. Consequently, a main objective of the work was to validate the proposed TBM against reconstructed crash data (specifically, GIDAS data). The validation included sensitivity analyses and a comparison of TBM's delta-v with GIDAS and that of a simple brake-light-onset-based crash-causation model (BLOM). However, limitations of the validation process emerged during the work, creating a second main project objective: to propose a method to account for the selection bias in the GIDAS delta-v data when used for validation of baseline generation. A final secondary objective was to compare the outcome delta-v after an AEB was included (as 'treatment') in both sets of simulations (those based on the original crash data and those based on the TBM).

The primary metric used to assess and compare models was delta-v, calculated based on the relative speed at impact, vehicle masses, and conservation of momentum (see Appendix B for a detailed description of how delta-v is estimated in his work). Thus visualizations of the delta-v distributions are the primary means of comparison, but delta-v mean and other distribution-related summary metrics are also used.

## **2 Method**

### **2.1 Data and data pre-processing for scenario generation**

This study used three different types of data to generate crashes: crash kinematics data, glance behavior data, and driver pre-crash deceleration data. The three types and the pre-processing performed for each are described below.

#### **2.1.1 Crash kinematics data (from the GIDAS database)**

These data were collected from road traffic crashes from two metropolitan areas in Germany, Dresden and Hanover (Otte, 2003; Schubert, 2013). For a crash to be included, at least one person must have been injured as a consequence of the crash. Each case is entered into the database with codes for all the information from the crash investigator's compilation (e.g., police report, photos, vehicle data, hospital information, and interviews or surveys of the precrash phase). GIDAS also offers a subset of cases in a time-series format, a pre-crash matrix (PCM). In these cases the following vehicle's trajectories and acceleration profiles for the five seconds leading up to the collision are reconstructed in 10ms steps. The PCM data used in this study were purchased by Volvo Car Corporation (VCC; which regularly purchases a subset of both GIDAS and PCM data). All processing and handling of GIDAS data were done by VCC employees.

The preliminary criteria for selecting GIDAS cases in this study were: 1) PCM data is available and 2) the conflict situation corresponds to the “rear-end frontal” GIDAS crash type, defined by the Volvo Safety Center as a following vehicle crashing into a lead vehicle, when both are traveling in the same direction in the same lane. Data from the years 2008-2022 were selected and all crashes that fulfilled the above criteria were included.

The crashes were then further filtered using the following criteria: a) no lateral (steering) avoidance maneuver; b) no identified intention to overtake or change lanes; c) no on- or off-ramp nearby; d) the following-vehicle was not in a crossing; e) speed limit >50 kph; f) daylight, dusk, or dawn; and g) road was dry, damp, or wet.

All cases that fulfilled the above criteria were included, except for six cases which either had quality issues in the PCM or which were outside the range of technical limitations in the simulation methods, resulting in a total of 103 rear-end frontal crashes and were consequently used for this study.

### **2.1.2 Glance behavior data from SHRP2 and VCC (naturalistic driving studies)**

Two sets of off-road glance-behavior data from baseline driving were used in this study: a) data from an internal VCC study (hereafter called the Kungälv study; see Bärngman & Victor, 2019 for details about the glance data) and b) data from the Second Strategic Highway Research Program (SHRP2) Naturalistic Driving Study (Blatt et al., 2015). Descriptions of these datasets follow. Note that off-road glance data from the Kungälv study was used as the primary glance data source, while the SHRP2 data was used for a sensitivity analysis (i.e., to check how the specific baseline glance distributions affect the delta-v of the generated baseline crashes).

The Kungälv study was conducted on a main highway in the Gothenburg area. Twenty participants (9 women and 11 men) aged 27 to 62 drove a Volvo MY2016 XC90 between Gothenburg and Kungälv, conducting a set of self-paced visual manual tasks during the drive. The participants, recruited through emails sent to Volvo employees, were required to meet certain criteria—such as having a minimum of 5000 kilometers of driving experience in the previous year and not being involved in vehicle development or working as test drivers. In the original study, visual manual tasks at different levels of automation were performed. However, the current study, designed and conducted afterwards, used only the baseline data collected during manual driving. That is, for each driver, a 40-second data segment, starting 30 seconds after the completion of the last task, was used as the baseline.

The glances from the Kungälv data were manually coded, frame-by-frame, as located either on- or off-road. Glance transitions and blinks were coded as part of the previous glance (whether on- or off-road). However, if the glance was moved from on-road to off-road during a blink, the blink was considered part of the following off-road glance instead. The duration of all off-road glances (for all drivers) were put into bins with a width of 0.1 s, while the total

proportion of time the drivers looked on the roadway added as a point mass at the off-road glance duration of zero (i.e., a single point in the distribution). The data are shown in Figure 1.

The SHRP2 data were obtained from the SHRP2, the largest in-vehicle naturalistic driving study conducted to date (Blatt et al., 2015). During this study, 3247 primary participants drove instrumented vehicles in their everyday lives across six sites in the US, covering a distance of almost 80 million kilometers over a two-year period. The recordings captured not only everyday driving but also nearly 7000 near-crashes and over 1000 crashes (severity levels 1-3; see (VTTI, 2015)). The present study used driver glance data manually annotated from a subset of everyday driving data from the Victor et al. (2015) study. Specifically, the off-road glance behavior data of the baseline epochs (segments 30s long) were extracted to match the SHRP2 rear-end crashes and near-crashes used in the Victor et al. study. A total of 1791 epochs (segments of time), with a total of 4604 off-road glances, were obtained.

The glance behavior information from the SHRP2 data was extracted in the following way: The driver's glance direction at a given time step was given by a discrete signal, with each value corresponding to a specific location (e.g., "Forward", "Instrument Cluster", or "Cellphone"). The driver's glance was considered to be on-road when the glance location was coded as either "Forward" or "Left windshield", and off-road otherwise. Glance transitions and samples corresponding to eyes closed, as well as short sequences (< 1s) of invalid values were concatenated to the previous glance (whether it being on- or off-road). Long sequences (> 1s) of invalid values were instead substituted with a single on-road glance sample, to avoid introducing too much uncertainty in the glance location data and to ensure separation of off-road glances. The durations of all off-road glance sequences were collected and sorted into bins of 0.1s each. The data are shown in Figure 1. Note that the point mass at zero in the probability density function (PDF) is the proportion of the time during baseline driving that the drivers had their eyes on the road.

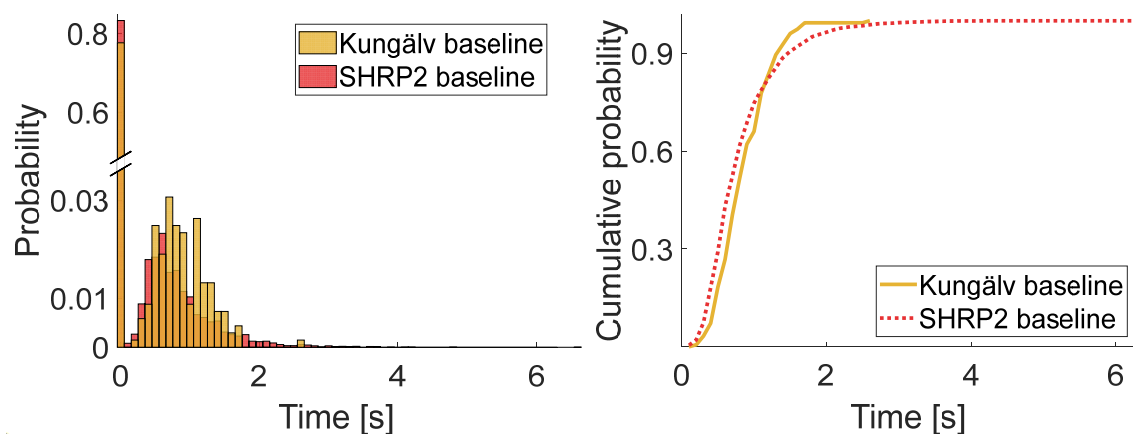


Figure 1. The empirical probability density function of the off-road glance durations with a point mass at zero used in the study (left), and the cumulative density function of the same.

Note that the point mass at zero in the left panel was so much larger than the other part of the distribution that a split was needed.

### 2.1.3 Driver pre-crash deceleration data from SHRP2 (naturalistic driving study)

While the onset of braking is modeled as in previous studies, the pre-crash braking behavior (i.e., not when but how hard the driver brakes) is described by a (more or less) fixed jerk and a distribution of maximum deceleration from real crashes.

In the simulation environment (using esmini Knabe (2023) as basis, with an external controller containing the driver, vehicle dynamics, sensors and the ADAS), the deceleration was controlled by applying a brake pedal force. As the method required the target deceleration to be available, the relation between deceleration and brake pedal force was identified empirically and mapped in the simulation software. In the simulation environment the jerk was controlled by applying a ramp-up of the force with which the driver pressed the brake pedal in the simulation environment. A mean jerk of  $-23.04 \text{ m/s}^3$  was determined empirically. There were some fluctuations in jerk across the deceleration range, resulting in a standard deviation of  $0.74 \text{ m/s}^3$  over the desired deceleration range. The same jerk was applied irrespective of the targeted deceleration.

The maximum deceleration was described by an empirical distribution extracted from 45 rear-end crashes in the SHRP2 data (see Figure 2). The dataset came from the Victor et al. (2015) study and the maximum deceleration was extracted from each case by fitting a piecewise linear model to the longitudinal acceleration data from each crash (see Figure 1 and Figure 2 in Markkula, Engström, Lodin, Bärghman, and Victor (2016), for examples). Only crashes with a maximum braking plateau were included, to ensure they genuinely contain the drivers' maximum deceleration. That is, crashes in which the deceleration was still increasing at the time of the crash were excluded.

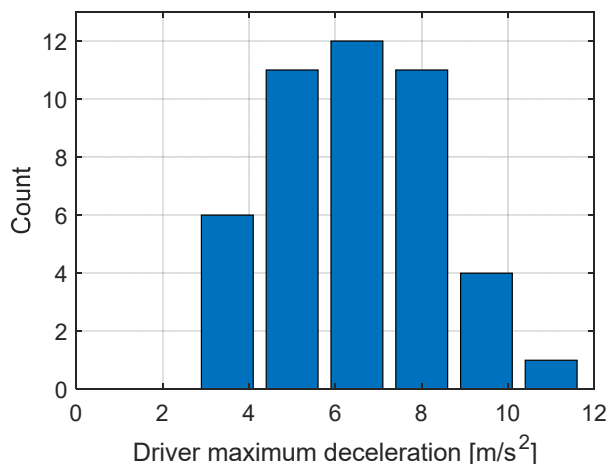


Figure 2. The empirical maximum driver deceleration from 45 SHRP2 crashes used in this work

## 2.2 The TBM's four sub-models

The TBM that this study aims to validate consists of four sub-models. The first, Off-road glance, is based on a response delay to a lead-vehicle conflict due to the following vehicle driver's off-road glances. The second, Too-close, is based on drivers who are driving too closely to the lead vehicle. The third, Low-deceleration, reflects a driver's failure to brake at the maximum deceleration possible (given the vehicle and road conditions). The fourth, No-response, relates to sleepy drivers. These sub-models are described in turn below. Note that the first sub-model, in addition to describing the crash-causation model, also includes a description of the model of the driver brake onset response, while the third sub-model includes a description of braking control (how the driver brakes).

### 2.2.1 Sub-model 1: Off-road glance behavior-based crash-causation and response onset model

This sub-model quantifies how drivers' glances off-road limit their ability to respond to a looming lead vehicle in time to avoid a crash. The off-road glance itself creates a response delay, based on the fact that the driver of the following vehicle is not looking at the lead vehicle, which in this scenario is on the road in front. When the driver does look back at the road, there is a further perception-action delay. This delay includes detecting the looming lead vehicle, moving the foot from the accelerator pedal to the brake pedal, depressing the brake pedal, and any subsequent delay due to the mechanics of the vehicle (e.g., brake pressure buildup and brake pad movement). See Figure 3 for an illustration of the glance application process.

The sub-model assumes that drivers do not accumulate information about the lead vehicle when they are looking away from the forward roadway. Note that this is a simplification, as studies have shown that the eccentricity of the off-road glance (i.e., how great the angle is that represents the difference between looking at the road ahead and the driver's actual glance direction) affects the time it takes for the driver to respond after looking back at the road (Svärd, Bärgrman, & Victor, 2021).

The specifics of the sub-model are based on the work presented in Markkula et al. (2016), which shows that drivers who look away from the roadway but look back again after  $\tau^{-1}=0.2s^{-1}$  respond very fast, with an average response time of just below 0.5s.  $\tau^{-1}$  is defined using the angle that the width of the lead vehicle subsumes on the driver's retina ( $\theta$ ) and its derivative ( $\dot{\theta}$ ) as  $\tau^{-1} = \frac{\dot{\theta}}{\theta}$ . It is the inverse of the optically defined time to collision (from the following-vehicle's driver's perspective) and is a measure of conflict urgency. The  $0.2s^{-1}$  threshold is based on Markkula et al. (2016) (see Figure 4 in that paper). The response time is slightly dependent on the urgency of the situation, with an average of 0.42s—but a couple of hundred milliseconds slower in less urgent events (close to  $\tau^{-1}=0.2s^{-1}$  when the driver looks

back)—and a couple of hundred milliseconds faster at more urgent events (larger  $\tau^{-1}$ ). However, in this study we used a fixed response delay of 0.5s to denote the time it takes for the deceleration to start after the driver looks back at the road.

The Markkula et al. (2016) study also shows that if a driver looks back on the road before  $\tau^{-1}=0.2s^{-1}$ , there is no correlation between urgency and response time. One interpretation of these two findings—an interpretation that we use in our TBM—is that only glances that overlap  $\tau^{-1}=0.2s^{-1}$  are relevant for crash-causation. If the drivers look back earlier, they will respond no later than  $\tau^{-1}=0.2s^{-1}$ , while if they look back at  $\tau^{-1}>0.2s^{-1}$ , they will respond immediately (after the 0.5s response delay). After  $\tau^{-1}=0.2s^{-1}$ , drivers will not look away, as the event is too critical (and they will have already initiated braking).

This interpretation also means that only the portion of the off-road glance that extends beyond  $\tau^{-1}=0.2s^{-1}$  is relevant for crash-causation (see Appendix C for more details). Consequently, to investigate the impact that different off-road glance behavior “counterfactually” would have on a specific crash, it is possible to virtually apply a specific distribution of off-road glance durations to that crash (see Figure 1 for an example of an off-road glance distribution for everyday highway driving). This is done by overlapping individual off-road glance durations with the time in the crash kinematics where  $\tau^{-1}=0.2s^{-1}$ , and then running simulations using the response model described above. It is possible to perform a statistical transformation of the original off-road glance distribution to what is called an overshoot distribution, and subsequently place (anchor) an overshoot glance from the overshoot distribution at  $\tau^{-1}=0.2s^{-1}$ . See Appendix C for a description of the overshoot distribution. In this study an overshoot distribution was used to reduce the number of simulations needed by a factor of approximately 30. Finally, note that before the glance behavior is added to the pre-crash kinematics, the speed of the evasive maneuver is removed from the following vehicle’s speed profile (see Figure 3), to allow for model-based counterfactual behaviors.

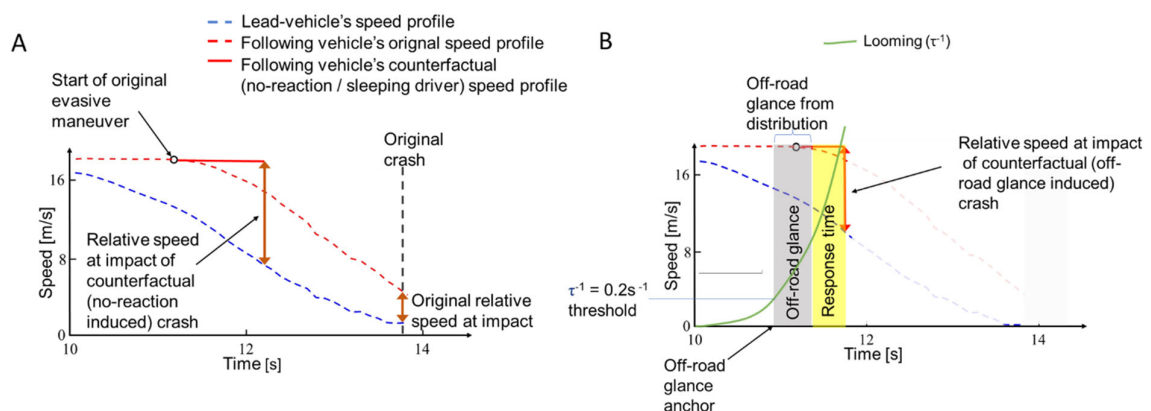


Figure 3: Overall application figure, with looming, threshold, glance application, delay/response time. Rear-end crash with original speeds and no-reaction counterfactual speeds (“what-if” the following vehicle did not react; left panel), and an off-road glance induced counterfactual crash (“what-if” the driver looked away; right panel) with a glance anchor at  $\tau^{-1}=0.2s^{-1}$ .

### **2.2.2 Sub-model 2: An attentive driver driving too close to the lead vehicle**

The second crash-causation sub-model was implemented simply by having the driver look on-road at all times. This is operationalized by including the point mass at zero in the off-road glance distribution (see Figure 1) when performing the simulations. The crashes then occur due to the combination of short time gaps between the lead and following vehicles in the original crash kinematics and the maximum deceleration of the driver in each individual simulation (see Simulations below for details).

### **2.2.3 Sub-model 3: Drivers not braking as hard as possible**

The third crash-causation sub-model reflects drivers' tendency to not brake as hard as possible, even if they are about to crash. The model's implementation is based on the distribution of drivers' maximum decelerations as described earlier. A previous study did not find any relationship between glance duration and maximum deceleration in the SHRP2 data (Bärgman et al., 2017). Therefore, sub-models 1 and 3 are assumed to be independent.

### **2.2.4 Sub-model 4: Sleeping or drowsy drivers**

The fourth and final crash-causation sub-model describes a sleepy (resulting in the driver not responding to the looming lead vehicle) driver. It was assumed that this mechanism contributes to approximately 10% of all rear-end crashes (somewhere in the middle of what is reported in Horne & Reyner, 1999; Knipling & Wang, 1994). This sub-model was operationalized in the simulations as no braking at all prior to crashing. Practically the delta-v distribution of the no-response crashes (one per original GIDAS crash) was added so that the total proportion of these crashes out of all simulated crashes was 10%. That is, the no-response crashes were added after the crashes of the other three sub-models were created. The no-response crashes were created by simulating each event without any reaction by the following-vehicle driver. Practically, the final delta-v distribution was obtained by calculating the weighted sum of the (normalized) delta-v distribution resulting from the three previous sub-models (90%) and the (normalized) no-response delta-v distribution (10%).

## **2.3 The brake-light onset model (BLOM)**

In addition to the validation of the TBM we also include a comparison between the TBM and a more traditional crash-causation model, in which a driver starts braking (with some reaction time) after the lead-vehicle's brake lights go on. We call this the brake-light onset model (BLOM).

The BLOM uses a simple driver reaction-time distribution and the same deceleration distribution as the TBM (see Figure 2). For each simulation a unique pair of reaction time ( $T_{\text{react}}$ ) and maximum deceleration ( $d_{\text{max}}$ ) from the distributions is used. In the simulation, the BLOM identifies the time point of the lead-vehicle start braking (the brake-light onset). It then waits

$T_{\text{react}}$  seconds, after which it starts braking with  $d_{\text{max}}$  (with the same variance on jerk and maximum deceleration as for the TBM; see 2.1.3).

We used the onset of the lead-vehicle braking as the reaction time onset, which is what most experiments measure when studying the impact on safety of a particular manipulation (e.g., when the driver is asked to perform a visual-manual or cognitive task (He & Donmez, 2022), or when assessing forward collision warning (Aust, Engström, & Viström, 2013)). However, using brake-light onset has its drawbacks, as for cases when the lead-vehicle is not braking at all or is standing still at the start of the event, the system would, depending on implemented logic, either not brake at all or brake fully directly at the start of the simulation, respectively. In this study we chose to exclude all cases that had these drawbacks to not unjustifiably classify a case as crash or avoidance, leading to a reduced dataset of 72 cases (38 excluded). This study used a log-normal reaction time distribution from Green (2000), with

$$\mu = \log\left(\frac{m^2}{\sqrt{v + m^2}}\right)$$

and

$$\sigma = \sqrt{\log\left(\frac{v}{m^2} + 1\right)}$$

where  $m = 1.275$  and  $v = 0.6^2$ . This distribution was for the purpose of simulations discretized into 26 bins, with a step size of 0.2s (from 0 to 5s), as shown in Figure 4. The distribution was cut as  $t = 5$  as the additional contribution of crashes beyond that is marginal.

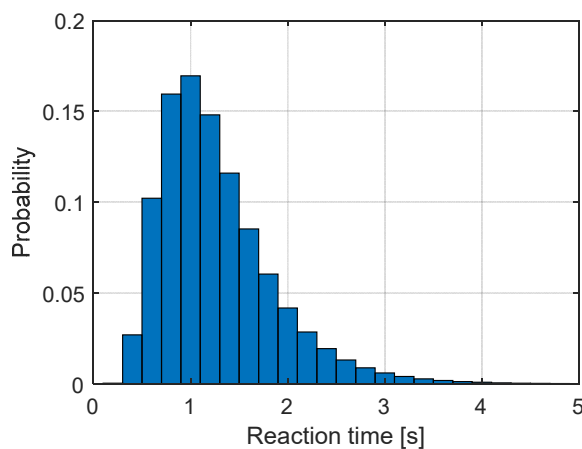


Figure 4: The discretized log-normal reaction time distribution used in the BLOM.

## 2.4 Automated Emergency Braking system

The AEB used in this study, which came from Volvo's own development work, does not represent production-ready software. That is, it contains unverified functionality and is not used in production cars. However, it is considered a reasonable representation of a modern AEB. Note that as this study only performed a relative comparison between the GIDAS data and the TBM, specific details about the AEB implementation should not be needed. (Moreover, it is proprietary intellectual property of Volvo Car Corporation).

## 2.5 Parameter selection, simulations, and simulation output

The simulations were based on the 103 original rear-end GIDAS cases. The evasive maneuver of the following vehicle was removed from each case, replaced with a constant speed. The first step for each individual simulation was to select parameters to be used in the simulation, including setting the off-road glance duration (from the overshoot-transformed baseline off-road glance distribution; see Figure 1) and the maximum deceleration (from the distribution shown in Figure 2). The off-road glance distribution was divided into 0.1s bins, creating a total of 27 bins for the Kungälv data and 67 bins for the SHRP2 data (as the longest glance is longer in the latter). The maximum deceleration was divided into 1.5 m/s<sup>2</sup> bins, creating a total of six bins. Nominally, for each original crash with the Kungälv glance data this resulted in 27 x 6 = 162 simulations. With a total of 103 original crashes, the nominal set of simulations for each simulation set was 103 x 162 = 16 686 simulations. A process to avoid running the same simulation more than once was adopted, substantially reducing the total number of simulations needed.

### 2.5.3 Simulation sets

Seven sets of simulations were completed for this study. Table 1 shows the details. In treatment simulations, the AEB system was applied to the baseline crashes. The 'Kungälv baseline' refers to the glance distribution collected for manual driving in Sweden, and the 'SHRP2 baseline' refers to the glance and deceleration distributions based on data from the SHRP2 project. 'Removed evasive maneuver' indicates whether the original evasive maneuver from the original conflict situation was preserved in the simulation. 'Reaction time' is for TBM the time from when the drivers had their eyes back on the road (after looking off-road) until they started braking (brake onset), and for BLOM the reaction time after the lead vehicle brake light onset.

Data/ model	Simulation type	Glance distribution	Deceleration distribution	Removed evasive maneuver	Looming threshold [1/ $\tau$ ]	Reaction time [s]
GIDAS	Baseline	N/A	N/A	No	N/A	N/A
GIDAS	Treatment	N/A	N/A	No	N/A	N/A
TBM	Baseline	SHRP2 baseline	SHRP2 baseline	Yes	0.2	0.5
TBM	Baseline	Kungälv baseline	SHRP2 baseline	Yes	0.2	0.5
TBM	Treatment	Kungälv baseline	SHRP2 baseline	Yes	0.2	0.5
BLOM	Baseline	N/A	SHRP2 baseline	Yes	N/A	Green*
BLOM	Treatment	N/A	SHRP2 baseline	Yes	N/A	Green*
TBM	Baseline	Kungälv baseline	SHRP2 baseline	Yes	0.3	0.5
TBM	Baseline	Kungälv baseline	SHRP2 baseline	Yes	0.2	0.8

\* Green here means the glance distribution from Green (2000), also described in section 2.3.

*Table 1: The simulation sets*

### 2.5.3 Calculation of delta-v

We did not have enough information for the simulations to calculate the true change in speed during the crash of the involved vehicles (the typical definition of delta-v; see Wang, 2022). Instead, we used a process to convert the relative speed at impact, using the masses of the involved vehicles and assumptions about conservation of momentum. The details of how this delta-v was calculated for each simulated crash are provided in Appendix B, and further description about the validity of this calculation compared to GIDAS estimates of delta-v can be found in Appendix D.

### 2.6 Prevalence weighting of simulation crashes

When performing simulation-based virtual safety assessment, care needs to be taken to make the crashes resulting from simulations represent the original crashes. Specifically, each of the 103 original (seed; as they are the origins of the created crashes) GIDAS crashes typically generated a set of simulated crashes (see Figure 5). Since each simulation crash with the TBM added can generate a different number of counterfactual crashes, the generated crashes must be prevalence-weighted so that the simulated crashes for a particular seed crash represent only the individual seed crash. That is, an original crash that results in 10 simulated crashes should contribute to the overall outcome impact speed distribution to the same extent as an original crash that results in 100 simulated crashes. Appropriate prevalence weighting means that the contribution of each of the 10 simulated crashes contributes 1/10, and each of the 100 simulated crashes contributes 1/100. Note that this balancing should be “on top” of accounting for the glance- and braking probabilities. The weighting was consequently accomplished as follows:

- a. For each original crash, sum the probabilities of the combination of the glance and deceleration across all the simulations that ended up as crashes. Denote these sums as  $q_1, \dots, q_N$ , where  $N$  is the number of original crashes.
- b. Normalise the probabilities so that  $q_1 + \dots + q_N = 1$ .  $w_i = 1 / q_i$ .
- c. Re-weight the generated crashes by a factor  $w_i$ : for each original crash  $i$  and generated crash scenario  $j$ , use the weight  $w_i p_j$ , where  $p_j$  is the probability glance and deceleration of simulation  $j$ . Note that the sum of  $w_i p_j$  at the end should be normalized to one.

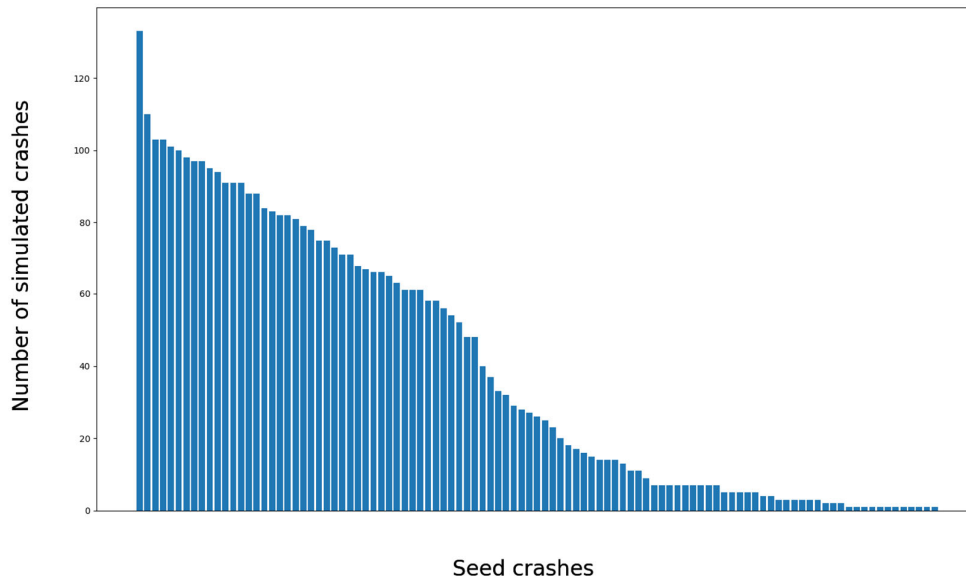


Figure 5: The number of simulated crashes based on the TBM for each original (seed) GIDAS crash, sorted in descending order.

## 2.7 Preparing for the comparison between GIDAS original and simulated data

A core part of validating a TBM such as the one proposed in this paper is to check whether the two datasets have the same underlying sample selection mechanisms—and if they do not, to ensure that any selection bias is compensated for.

This section describes a process to improve the validity of comparisons between simulated and actual crashes, when the latter are obtained from crash databases with selection bias (as in this case, since PDO crashes are not included). Note that the process includes many assumptions, which are likely to impact the overall validation relevance; accordingly, they are listed below. We are, however, demonstrating the importance of performing this correction in order to validate crash-causation models.

First, we sought to represent all rear-end PDO crashes by creating an analytical PDO distribution. We used insurance data with some (albeit censored) PDO data, and complemented the resulting distribution with an assumption about its shape as well as information from the literature. Using this distribution, we then added PDO data to GIDAS data, to achieve a GIDAS-with-PDO distribution. Finally, we estimated the parameters for an analytical transfer function that converts the GIDAS-with-PDO distribution to the original GIDAS data. We later also used this function to transform the delta-v distributions generated from simulations (which should include crashes on all levels of severity), in order to have the same sample selection as GIDAS. Details of this process are given below.

### **2.7.1 The Folksam data**

The Folksam data come from insurance claims from vehicles with event data recorders (EDRs) which were installed by the insurance company for research purposes. The data has an inclusion threshold of 50,000 SEK (before 2012) and 70,000 SEK (from 2012) in repair costs (i.e., only crashes with repair costs above this are included in the data used in this study).

The data available for this study were at the occupant level only (not at the crash or vehicle level) and included MAIS levels 0-6 for each individual involved in the crashes for which data were collected. For each individual, only max MAIS was available. For frontal impacts, only data for the driver and any front seat passenger were available. (See Ydenius et al., 2013, for more details about the data). A total of 912 data points (individuals) with MAIS 0-6 coding and the corresponding estimated delta-V were available; whether the individual was a driver or a passenger was also specified.

In total, 43% of the individuals in the dataset had no injury (MAIS0); the remaining had injuries ranging from MAIS1-6. See Panel A in Figure 6 for the distribution of all crashes, and panel C for the distribution of MAIS0 individuals.

### **2.7.2 Data on the overall proportion of rear-end crashes with property damage only (PDO)**

Studies have estimated the proportion of PDO crashes out of all crashes across all severities. One of the most cited sources on rear-end crashes is Knipling et al. (1992), which estimates that between 70% and 75% of all rear-end crashes incur property damage only (see Appendix A for details). We use 70% in the PDO correction process in this work. However, a sensitivity analysis was performed to assess the impact of the choice of the overall proportion of PDOs in the data. The range 55% to 85% (i.e., 70%  $\pm$ 15%) with a step size of 5% was assessed.

### **2.7.3 Estimating the data censored by the repair-cost threshold**

The intention was to create a complete PDO delta-v distribution, as accurate as the information currently available allows. Given the estimates of the total proportion of rear-end PDO crashes (70%) and of the proportion and delta-v distribution for the Folksam data (43%), we calculated how much data need to be added to the Folksam data to create a dataset representing all PDO cases, and where in the distribution they should be added.

- Step 1. Stating assumptions:
  1. Assume that repair cost is proportional to delta-v
  2. Similarly, assume that, for rear-end crashes in general, there are fewer crashes as delta-v increases.
  3. From these assumptions it follows that the PDO crashes should be added to the Folksam data at the lowest delta-vs. It is also likely that the vast majority

of the PDO data should be added below the mode of the Folksam PDO data (see Panel C in Figure 6).

4. Let  $P_{PDO}=0.7$
  5. Let  $N_{Folksam\_PDO}=0.43$
- Step 2: Creating the PDO distribution:
    1. Identify the mode of the original Folksam PDO.
    2. Calculate how much data should be added to the Folksam PDO data to create a full PDO distribution.
      - i. The total count of PDO should be
 
$$N_{PDO\_total} = (N_{Folksam\_MAIS0-6} - N_{Folksam\_PDO}) / (1 - P_{PDO})$$
      - ii.  $N_{Folksam\_PDO\_to\_add} = N_{PDO\_total} - N_{Folksam\_PDO}$
    3. Choose an analytical PDF form to be fitted to the full PDO data. Here we chose  $f(\Delta v) = B_1/e^{(B_2 * \Delta v)}$ .
    4. Manually add  $N_{Folksam\_PDO\_to\_add}$  at and below the mode of the original Folksam PDO so that it “looks like” the chosen functional form.
    5. Find the parameters  $B_1$  and  $B_2$  that give the best fit.
    6. If the manually added  $N_{Folksam\_PDO\_to\_add}$  does not create a good fit, return to Step 4., modifying the proportion across the lower bins until a satisfactory fit is obtained in Step 5.

The output (Panel E in Figure 6) is consequently a best guess of the shape of the true PDO. Note that it does not have to be perfect—it is the approximate shape of the PDO distribution that is of interest, so that the GIDAS data is transformed to include PDO crashes.

The final equation describing the full PDO distribution is:

$$f(\Delta v) = 0.18/e^{(0.09 * \Delta v)} \quad (\text{Eq. 1})$$

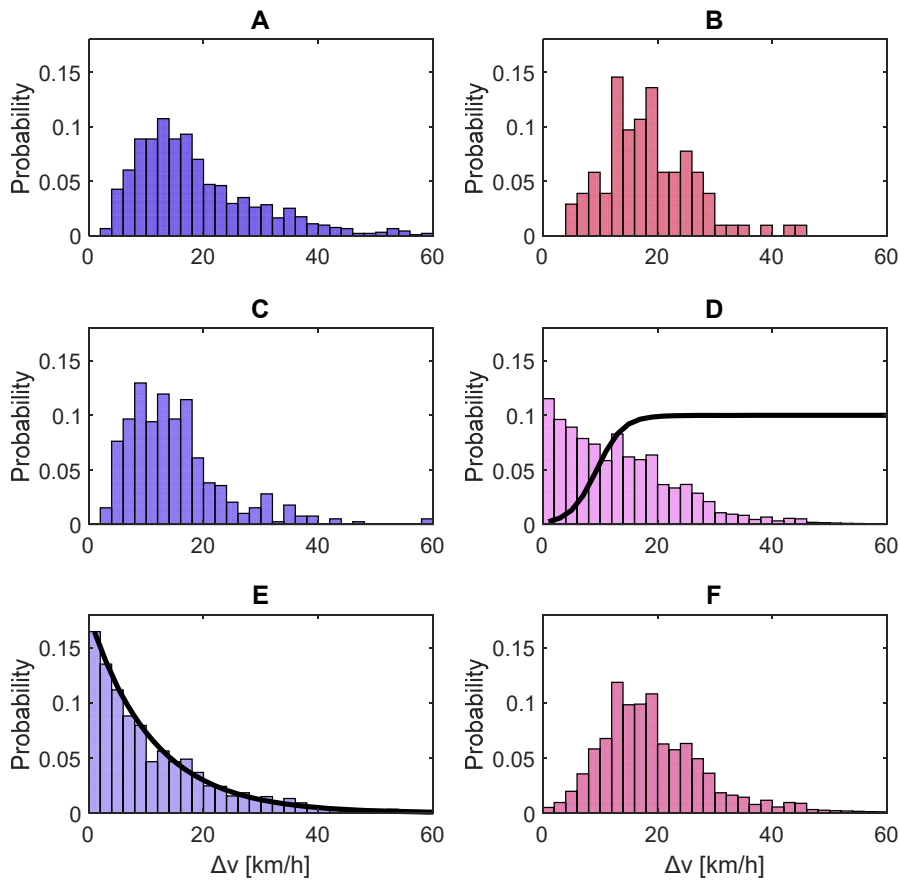


Figure 6: The steps included in the creation of a transfer function from rear-end delta-v distributions that include all levels of severity to a delta-v distribution censored in the same way as GIDAS: Folksam data with 43% property damage only (PDO) crashes (Panel A). Folksam PDO data only (Panel C). Folksam PDO with data manually added at the lowest four bins to that the total becomes 70% (complementing the 43%) to create an exponential decline, and an exponential fitted (Panel E; Eq. 1). Original GIDAS crashes (Panel B). Original GIDAS with data added per the fitted exponential in Panel E to make the total PDO 70%, including a transfer function (Eq. 2) to transform the data in Panel D to mimic the GIDAS sample selection. Panel F shows the outcome of the application of the transfer function (black line in Panel D) to the histogram in Panel D.

#### 2.7.4 Adding the PDO data to the GIDAS data

As the GIDAS data (ostensibly) only include injury data, we can add the PDO data (with the shape of the final equation in the last step) to the GIDAS data, with a proportion of PDO crashes from the literature (e.g.,  $P_{\text{PDO}} = 0.7$ ). That is, we add data per Eq. 1 (see panel E in Figure 6) to the GIDAS original data (panel B in Figure 6), so that the proportion of PDO crashes are 70% of the total. The result can be seen in panel D in Figure 6.

### 2.7.5 Transforming the GIDAS data with PDO back to the original GIDAS data

The inclusion mechanism of GIDAS should now be the transform from the GIDAS with PDO (panel D in Figure 6) to the original GIDAS (without PDO; panel B in Figure 6). Such a transformation can be done in several ways, but here we chose to find  $C_1$  and  $C_2$  in

$$P_{\text{MAISO-6\_to\_MAIS1-6}}(\Delta v) = e^{(C_1+C_2*\Delta v)} ./ (1 + e^{(C_1+C_2*\Delta v)})$$

by minimizing the cost function

$$\text{cost} = \text{sum}(\text{GIDAS}_{\text{original}_i} - \text{GIDAS}_{\text{withPDO}_i})$$

by an exhaustive search of  $C_1$  and  $C_2$  (with the ranges -10 to -0.1 in 0.05 steps, and from 0.001 to 5 in 0.001 steps, respectively), and where

$$\text{GIDAS}_{\text{withPDO}_i} = \text{GIDAS}_{\text{original}_i} * P_{\text{MAISO-6\_to\_MAIS1-6}}(\Delta v_i)$$

The resulting transfer function is

$$P_{\text{MAISO-6\_to\_MAIS1-6}}(\Delta v) = e^{(-4.1 + 0.437*\Delta v)} / (1 + e^{(-4.1 + 0.437*\Delta v)}) \quad (\text{Eq. 2})$$

Note that any transformed distribution should either be normalized (to probability) or re-weighted (to the original number of cases). Equation 2 is shown as a sigmoid in Figure 6, Panel D. The application of that function to the distribution in Panel D is shown in Panel F. The distributions in Panel B and Panel F should now be similar, which they seem to be.

It should now be possible to use  $P_{\text{MAISO-6\_to\_MAIS1-6}}(\text{delta-v})$  directly to convert distributions created using crash-causation models that produce data across all severities (including MAISO/PDOs), to mimic the GIDAS sample selection process.

## 2.8 Analysis

### 2.8.1 Comparison across GIDAS and models

Most comparisons are made by visualizing the complete empirical distribution of the delta-v of two simulation sets. The mean of the distribution is typically included in the figures. In Appendix D we also present statistics for some of the distribution comparisons.

Note that for most of the metrics several weighting steps are needed (i.e., case/pro propensity weighting, selection bias transform, and the probability that each case would occur, given the off-road glance and maximum deceleration probability). These steps are described in each respective method description.

## **2.8.2 Validation data selection bias**

We apply the injury risk functions for MAIS1+, MAIS2+, and MAIS3+ to the distribution of crashes from the TBM and to the same distribution transformed to mimic the GIDAS sample selection. The purpose is to compare the results, in order to investigate how the selection bias affects the calculation of injury risk.

The injury risk functions used were those for frontal crashes reported in Wang (2022; Table 1.1). Note that, to keep this part of the work less complex, we did not consider the combination of rear-end injury risk and frontal injury risk that are part of a rear-end crash. Instead, we only considered the frontal impact injury risk.

## **3 Results**

This study includes four main analyses. First, we compared the delta-v distributions of the original crashes generated from GIDAS, TBM, and BLOM. We then made the same comparisons after AEB was applied, followed by an analysis of the impact of the selection bias on injury risk calculations. Finally, we performed four sensitivity analyses.

### **3.1 Comparing delta-vs for crashes generated from GIDAS, TBM, and BLOM**

The main validation in this study is based on a comparison of the estimated delta-v of the 103 original GIDAS crashes and the TBM-generated crashes. The comparison was made possible by transforming the latter using Eq. 2, to mimic the GIDAS sample selection process (see Figure 6).

The top panel in Figure 7 shows that the mean delta-v of the original TBM crashes, without sample selection transformation, is at 10.31km/h much smaller than that of the GIDAS crashes, with a very large proportion of crashes at low delta-v. This is expected, as the simulations should produce crashes across all levels of severity, without the bias present in in-depth crash databases.

More importantly for model validation, however, it shows that the delta-v ( $M=15.53\text{km/h}$ ; middle panel, Figure 7) of the transformed distribution is relatively similar to that of the GIDAS distribution ( $M=18.5\text{km/h}$ ). The distribution of the TBM-generated crash is shifted approximately 3km/h towards lower severities. The main difference between the TBM and GIDAS is that the GIDAS data has more crashes from 15-30km/h delta-v, while the TBM has more at 12-18km/h. We also compared the distributions using a range of other summary metrics but leave that for enthused readers – see Appendix E.

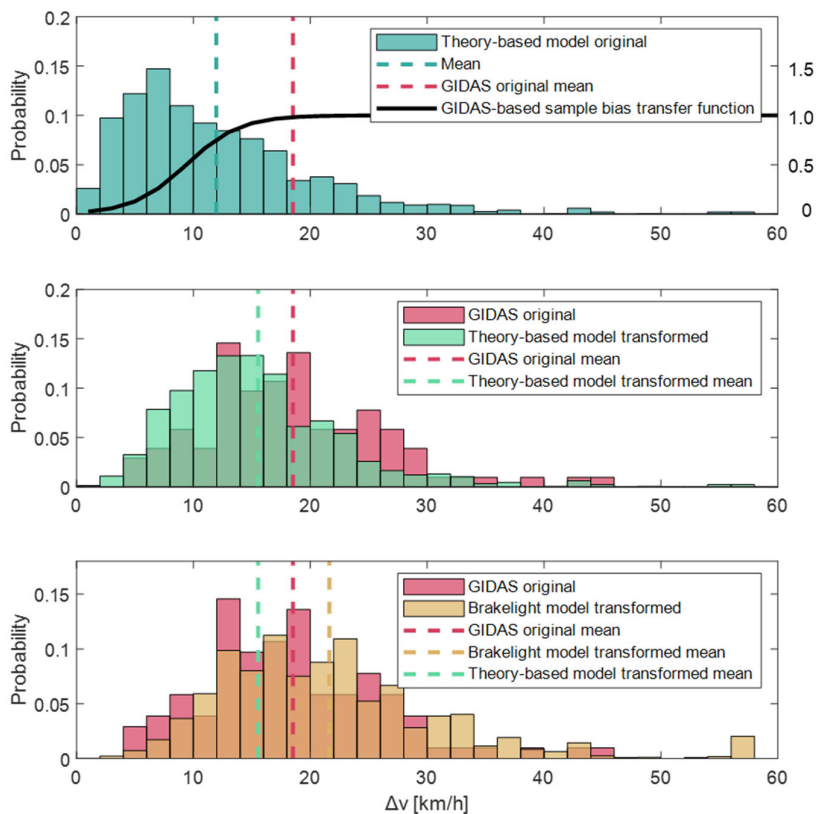


Figure 7: A comparison between the original GIDAS cases and the scenarios generated using the proposed TBM and the BLOM. The top shows the actual crashes generated by the TBM (without transformation), while the middle panel shows the normalized distribution from the top panel after Equation 2 (shown as the solid sigmoid in the top panel) is applied – that is, the distribution in the top panel has been transformed to mimic the GIDAS sample selection process. The bottom panel shows a comparison between GIDAS and the BLOM-generated crashes.

In addition to comparing the TBM to GIDAS, we made a comparison with the performance of a brake-light onset (BLOM) crash-causation model. The bottom panel of Figure 7 shows that instead of underestimating delta-v (as TBM does) the BLOM overestimates delta-v (a little more than TBM underestimates it). Note that as the BLOM does not handle cases when the lead vehicle is not braking or is at a standstill, such cases (38 out of 103; 36.9%) were excluded from the BLOM simulations (and are thus not part of the bottom panel in Figure 7).

Figure 8 shows the number of crashes generated in the baseline generation per original (seed) GIDAS crash. Here the “white” part in the bottom panel is the 36.9% of the BLOM crashes that are not included. The figure also shows the difference in number of generated crashes per seed crash, where the BLOM has a lower maximum number (130 vs 70) and the shape is different (i.e., overall not such a large spread in the number of crashes per seed crash for BLOM).

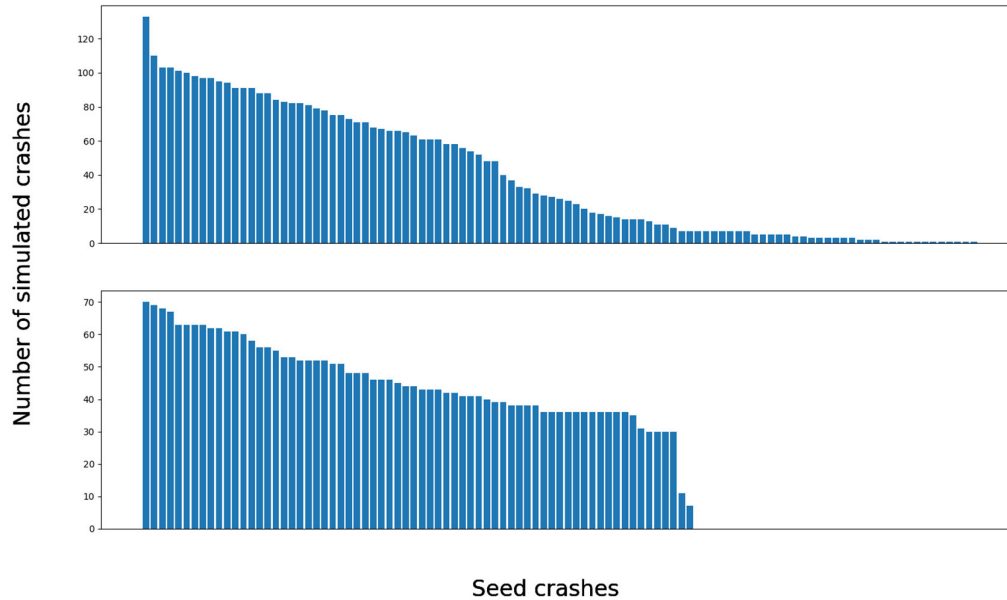


Figure 8: The number of crashes generated in the baseline generation, per original (seed) GIDAS crash, for the TBM (top panel) and the BLOM (bottom panel). Note that the missing values bars for the BLOM are the cases that were excluded because the lead vehicle either did not brake or was standing still at the start (in total 38).

### 3.3 Comparing TBD with GIDAS after application of AEB

We also applied the example AEB to compare the proportion avoided crashes and the delta- $v$  distributions of GIDAS data with the crashes generated by a) the TBM, and b) the BLOM. However, the AEB is very efficient, resulting in only seven crashes with AEB out of the 103 original GIDAS crashes. This means there are substantial uncertainties in any comparison. However, Figure 9 shows the in delta- $v$  distributions, and both the TBM and the BLOM substantially underestimates the effectiveness of AEB (but again, care should be taken when comparing with so few cases).

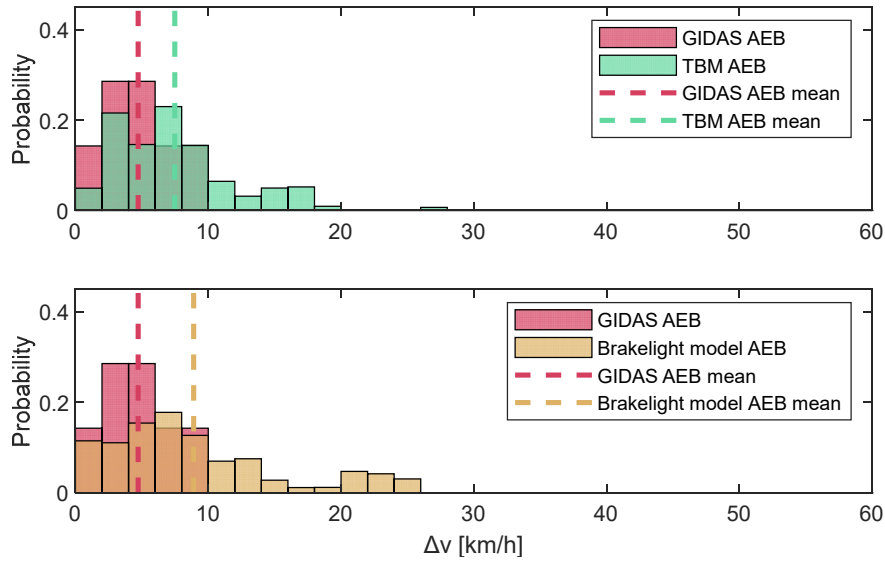


Figure 9: Comparison of delta-v after AEB was applied to GIDAS and TBM (top panel) and BLOM (bottom panel) baselines, respectively.

### 3.4 Validation-data selection bias

We have proposed a process for considering the selection bias of the dataset against which scenarios generated through virtual simulations are compared. Here we further investigate the impact of ignoring the bias when estimating injury risks. Specifically, we investigate the differences in terms of injury risk for MAIS1+, MAIS2+, and MAIS3+, by applying the three injury risk functions to the non-transformed virtual simulations and to the transformed simulations and comparing the results. Based on the dose-response model (Kullgren, 2008), we calculated the estimated proportion of injuries at each injury risk level. That is, we determined the proportion injured at each injury risk level for GIDAS, for the original (non-transformed) TBM-generated crashes, and for the crashes generated by the transformed TBM. The calculation conducted is

$$I_{MAISX+} = \int_0^{\infty} R_{MAISX+}(\Delta v) \cdot h(\Delta v) \cdot d\Delta v$$

where  $I_{MAISX+}$  is the proportion injured for the level of injury,  $R_{MAISX+}(\Delta v)$  the discretized injury risk function for each respective level, and  $h(\Delta v)$  is the empirical delta-v distribution (i.e., GIDAS, the original TBM, and the transformed TBM crashes). Figure 10 shows the components in  $I_{MAISX+}$ , while Table 2 shows the proportion of injured individuals for all combinations. The transformed TBM is more similar to GIDAS than the original TBM is, across all levels of injury risk. However, more importantly, the original TBM underestimates the proportion of the TBM transformed by 11%, 17%, and 21%, respectively.

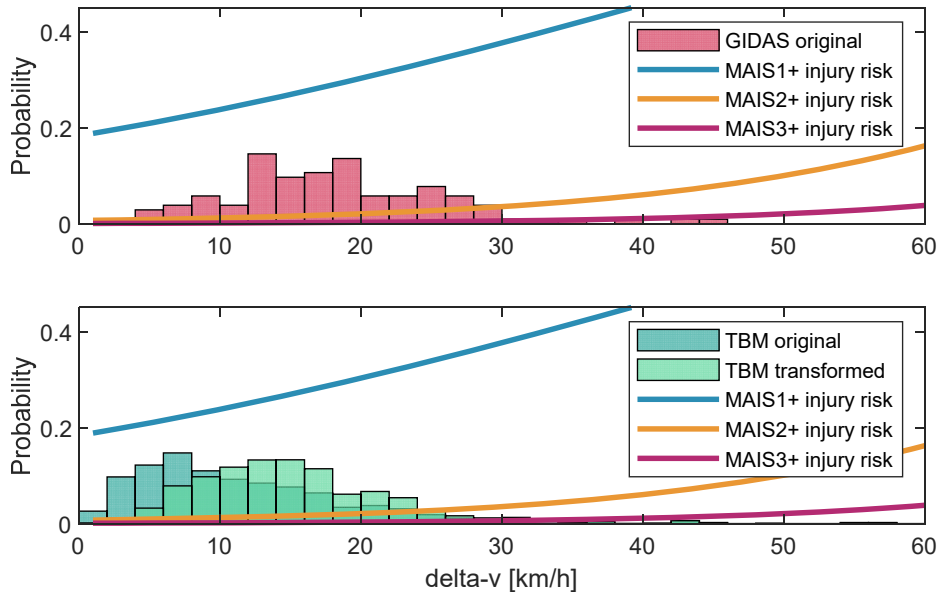


Figure 10: A visualization of the injury risk functions ( $R_{MAISX+}(\Delta v)$ ) and the models ( $h(\Delta v)$ ).

	$I_{MAIS1+}$	$I_{MAIS2+}$	$I_{MAIS3+}$
GIDAS	0.758	0.0894	0.0172
Original TBM baseline	0.608	0.0569	0.0111
Transformed TBM baseline	0.685	0.0685	0.0140

Table 2: The proportion of injured occupants across the different levels of injury, when applying MAIS1+, MAIS2+ and MAIS3+ injury risk functions to the original and transformed TBM delta-v distribution.

### 3.5 Sensitivity analysis

We performed four sensitivity analyses, comparing the delta-v distributions between a) two different off-road glance duration distributions (see Figure 1), b) two different  $\tau^{-1}$  thresholds (for glance anchoring;  $\tau^{-1} = 0.2^{-1}$  and  $0.3s^{-1}$ ), c) two different driver response times (0.5 and 0.8s), and d) a range of different assumption of the proportions PDO crashes in “real-traffic” (55% to 85% in 5% steps). The results are presented in turn.

As the top panel of Figure 11 shows, the two glance distributions have similar delta-v distributions, but where the SHRP2-glances shift the distribution slightly towards higher-severity crashes. Note that the number of crashes generated increases from 4059 to 9245 when the Kungälv glance distribution was replaced by the SHRP2 distribution.

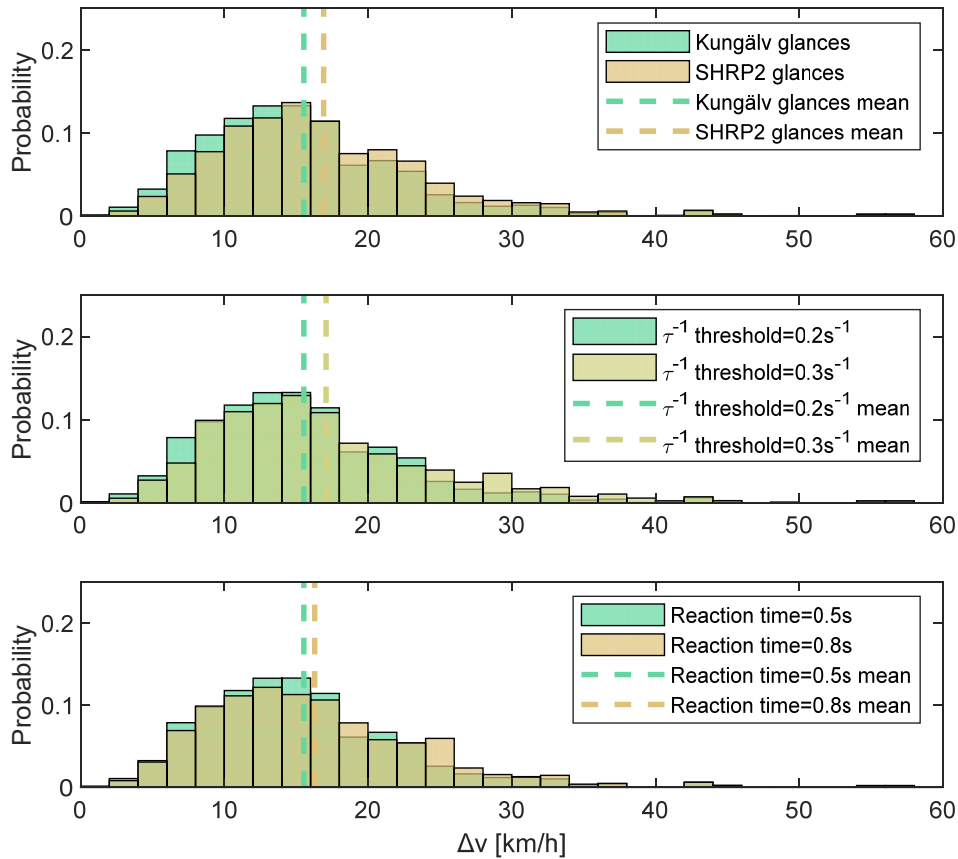


Figure 11: Comparison of delta-v for the baseline scenario generation using the SHRP2, and the Kungälv baseline off-road glance distributions (top panel), the TBM with two different  $\tau^{-1}$  thresholds ( $0.2s^{-1}$  and  $0.3s^{-1}$ ; middle panel), and for the TBM with two different response times ( $0.5s$  and  $0.8s$ ; bottom panel).

As the middle panel of Figure 11 shows, the  $\tau^{-1}$  threshold changed the delta-v distribution by an amount similar to that of the glance distribution change. With the larger  $\tau^{-1}$  ( $0.3s^{-1}$ ; closer to the crash than  $0.2s^{-1}$ ) there was a slight increase in higher-delta-v crashes.

As the bottom panel of Figure 11 shows, an increase in the driver response time from  $0.5s$  to  $0.8s$  shifted the distribution marginally towards higher delta-v. As expected, this shift is in the same direction, but smaller, than that of the  $\tau^{-1}$  threshold change.

The fourth and final sensitivity analysis was to assess the impact of the choice of overall proportion of PDOs in the creation of the selection bias transfer function. The range 55% to 85% (i.e.,  $\pm 15\%$ ) with a step size of 5% was assessed. Figure 12 shows the results, which indicate that the mean estimate of the delta-v distribution after the original TBM is transformed is relatively insensitive to the choice of the total proportion of PDOs (used when selection bias transform function), with only a range of approximately 2km/h difference when changing from 55% PDOs to 85% PDOs. In this study 70% PDOs were used when creating the selection bias transfer function for all other analysis.

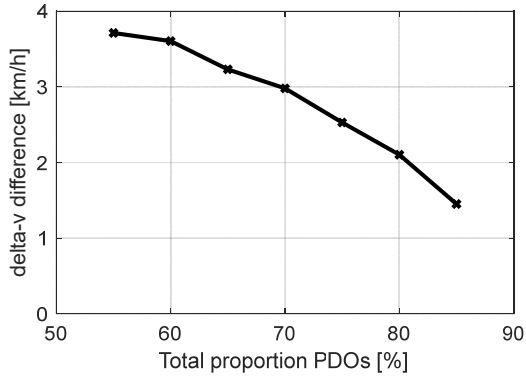


Figure 12: The difference between mean delta-v of the original GIDAS data and the transformed TBM.

#### 4 Discussion

In this work the primary aim was to validate a crash-causation, theory-based, baseline scenario generation model (called TBM), for use in the virtual safety assessment of ADAS and ADS, by comparing the model’s generated crashes against reconstructed crashes from the GIDAS database. The TBM has four sub-models, considering four different crash causation mechanisms: Off-road glances (delayed braking response due to off-road glances), Too-close (the following-vehicle is driving too close to the lead vehicle), Low-deceleration (the driver of the following vehicle is not braking as hard as is possible under the circumstances), and No-response (e.g., sleepy drivers). The validation was performed on the distribution of the estimated delta-v, as well as on summary statistics for the delta-v distribution.

In addition, the delta-vs for the TBM and GIDAS were compared after the application of an advanced AEB, the TBM was compared to a simple brake-light-onset (BLOM) crash-causation model, and four sensitivity analyses were performed (regarding the off-road glance distribution model choice, driver response time, and  $\tau^{-1}$ ).

Because GIDAS has a substantial selection bias (with PDO crashes excluded) and the TBM generates crashes at all levels of severity, it was necessary to devise a method to make valid comparisons between them. We created a transfer function that can transform a delta-v distribution of TBM crashes to a distribution with a selection bias similar to that of the GIDAS data. This step is important, as crash-causation-based baseline generation models like TBM typically produce crashes across all severity levels, while databases of actual crashes often have some form of selection bias.

##### 4.1 Comparing baseline delta-vs for GIDAS, TBM, and BLOM

Our results show that the proposed crash-causation theory-based baseline generation model (the TBM) creates crashes with a relatively similar delta-v distribution as that of the validation dataset (GIDAS), although the distribution is shifted some toward lower severity crashes,

compared to GIDAS. That the TBM creates a similar delta-v distribution with sub-models based on crash-causation theory is encouraging, as a theory-based model facilitates transparency in all steps of the virtual simulation process. As opposed to machine-learning based methods, such as those describe in Ding et al. (2023), when this kind of model is used in the assessment of a specific traffic safety solution (here, AEB, but it may be some other ADAS or ADS), it should be possible to dissect the benefits and drawbacks of the system. This analysis may reveal systemic issues and lead to the development of solutions. One such example is the assessment of systems which include the driver as part of the system, such as forward collision warning systems (FCW; Benmimoun et al., 2013). Studies have shown that drivers do not initiate braking directly based on the warning (other than in artificial laboratory settings, when told to do so); instead the FCW actually redirects the driver's gaze to the forward roadway (Aust et al., 2013). When on- and off-road glances are explicitly part of the crash-causation model (e.g., the TBM), glance redirections can be explicitly included in the assessment; thus the warning can be modeled to interrupt off-road glances (as well as sleepy drivers). When there are no explicit crash-causation mechanisms (e.g., in machine learning-based baseline generation, as well as in purely stochastic baseline generation without simulations ; Wimmer, 2023) it is far from obvious how to assess systems in which driver glance behavior plays a role.

We also assessed the performance of a much more simplistic crash-causation model, BLOM—which uses a simple reaction time (from a distribution) to the onset of braking of the lead vehicle. Results show that this model results in an overestimation of the delta-v just slightly larger than the underestimate by the TBM. The differences may be due to the inherent limitations of the BLOM approach. For example, studies have shown that drivers' braking responses to critical events are primarily driven by urgency, and much less by the onset of a lead-vehicle's brake-light. Although brake-light onset explains some of the variance in responses, it is not a good predictor for the start of braking of the following-vehicle in rear-end crashes (Markkula et al., 2016). Further, as previously mentioned, using brake-light onset is problematic (i.e., cannot be used) when the lead-vehicle is not braking, or at a standstill.

#### **4.2 Comparing AEB delta-vs for GIDAS, TBM, and BLOM**

As the main aim of virtual simulations often is to assess the performance of specific crash or conflict avoidance systems, and not just to create valid baselines, we applied a reasonably advanced AEB system to the three sets of baseline scenarios (GIDAS, TBM, and BLOM).

Results show that when AEB is applied, for both TBM and BLOM the mean delta-v is substantially larger than that of GIDAS. Note, however, that since AEB is so effective in avoiding crashes (only seven crashes remained of the 103), much care should be taken when interpreting the results, due to the uncertainties when comparing the mean of just a few crashes. Given the low number of remaining GIDAS crashes, it is not unlikely that some crashes generated by both crash-causation models would have been more difficult to avoid than the GIDAS original crashes – after all, the aim of scenario generation is to increase case coverage, trying to represent a more “complete” distribution than what the crash-database include.

### 4.3 Sensitivity analysis

We performed four sensitivity analyses in this study. The first assessed the impact of different baseline off-road glance duration distributions, showing that the choice of off-road glance behavior data does matter, but not a lot. That is, as expected, when the SHRP2 off-road glance data—with the longest glances being substantially longer than that of the Kungälv data—were used, the delta-v distribution was shifted slightly towards higher values. The large increase in the number of cases is likely due to the longer longest glances. Note that the distribution is so similar *in spite of* the large increase in crashes, which also indicate model robustness.

The sensitivity analysis related to the two model parameters and reaction time, results were in the expected direction, but smaller than expected. That is, when the TBM's  $\tau^{-1}$  was increased from  $0.2s^{-1}$  to  $0.3s^{-1}$  and when the reaction time was changed from 0.5s to 0.8s, the delta-v distribution was shifted towards lower-severity crashes, but for the reaction time only marginally, and also for  $\tau^{-1}$ , not much. That the changes were so small despite the increase in the total number of crashes from 4059 to 8613 with the  $\tau^{-1}$  increase, and 4059 to 4631 with the reaction time increase, is encouraging, as it indicates model robustness. Overall, these results indicate that the model is reasonably robust to changes in the a) glance distribution, b) glance anchor ( $\tau^{-1}$ ) threshold, and c) driver response time.

That there was only a small shift in the delta-v distribution when the glance distribution was changed may be an advantage for some forms of assessment, such as driver glance behavior assessments. Several studies have used a virtual simulation approach similar to the one used in this paper to assess the safety impact of driver glance behaviors (Bärgman et al., 2017; Bärgman et al., 2015; Lee et al., 2018), alone and in combination with different technologies (Bärgman & Victor, 2020). These studies have shown that there are substantial differences in outcome metrics across glance behaviors (off-road glance distribution, percent on-road glances, and task duration). The relatively low sensitivity to changes in the baseline distribution (what other glance behaviors is to be compared to; see e.g. Bärgman & Victor, 2020) should mean that comparisons to baseline are relatively robust.

Further, the comparison of off-road glance distributions in themselves is also interesting, as it compares baseline data from naturalistic driving data in the US with semi-controlled experiments on road in Sweden. Although there are differences, the cumulative density function shows them to be quite similar, except for the longer longest-duration off-road glances in SHRP2. However, this may simply be due to the SHRP2 data including more data.

### 4.4 The importance of considering sample selection bias in validations

Our results clearly demonstrate how the sample selection bias of the dataset against which simulation-generated baselines are validated can affect the validation's accuracy and precision (see Hautzinger, Pfeiffer, & Schmidt, 2005 for examples of GIDAS selection biases). Thus, performing validation using delta-v (or the equivalent, such as relative speed at impact) is clearly not advisable unless it is compensated for, as we propose. Otherwise, any simulation-

generated baselines that show good correlation with, for example, GIDAS, would include many more higher-severity crashes than the true distribution.

Our results also show that if models are validated on MAIS2+ or MAIS3+ injuries, the selection bias is not substantially reduced, compared to for MAIS1+. This is different from what we expected, which was that MAIS2+ and MAI3+ would be more similar between the non-transformed and the transformed TBM delta-v distribution, than MAIS1+. We expected the “bend” in the injury risk curve to basically remove the low severity crashes (similar to the transform we developed), but looking at Figure 10, all three injury risk curves are still relatively flat. This flatness of the injury risk curves over the range of the delta-v data in this dataset is likely the reason why the  $I_{\text{MAISX+}}$  for all three seems to be underestimating of the injury risk. This should be taken into account if injury risk functions are used “alone” (i.e., without a prior selection bias transformation, such as what we propose here).

As validation of crash-causation models for virtual safety assessment is rare, there is not much literature on the importance of considering sample selection bias in the validation of virtual safety assessment. Our results shows that this approach mitigates the issue but does not completely solve it. There is research on selection bias using crash databases (see Hautzinger et al., 2005 for an example on GIDAS selection bias), but not in the context of validating virtual simulations.

#### **4.5 The potential of tuning the TBM**

A relatively unique aspect of the crash generation process proposed through the TBM is that the model was not tuned to fit some outcome—instead, crash-causation theory and relevant knowledge and data about driver behavior were used to create the model. This information was enough to provide reasonably good validation results. It would certainly be possible to tune the model by tweaking its parameters (such as the  $\tau^{-1}$  threshold or the reaction time), but then it would no longer have a theoretically accurate basis. However, as the proportion of PDOs in real traffic (used in the creation of the sample selection transfer function) and of no-reaction crashes (in which drivers fail to react entirely) have large uncertainties, it may be that the corresponding parameters should be assigned values other than those used in this study. The model could potentially be tuned on these variables, modifying their values to reach a specific outcome—as long as realistic values are used. Figure 13 shows an example of such a tuning: the proportion of no-reaction crashes has been increased from 10% to 32%, so that the generated and original distributions now have the same means. This example probably represents an unreasonable number of no-reaction crashes (although Kusano & Gabler, 2012, used 29.5% in their work), but it demonstrates that tuning is possible—something that future research should look into.

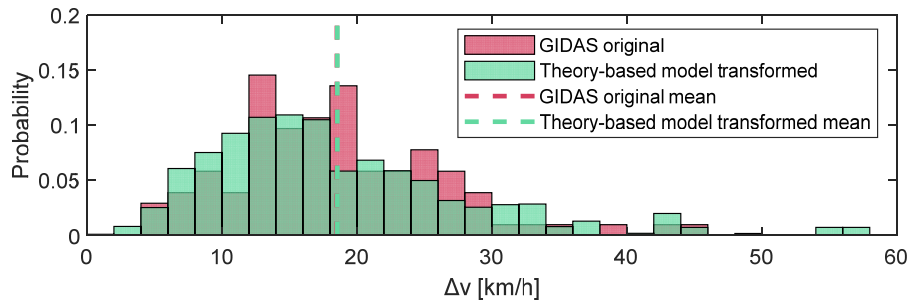


Figure 13: Results after tuning the TBM for the TBM mean to be the same as the GIDAS mean (they overlap).

#### 4.6 Limitations and future research

The limitations have been divided into four categories: those related to the creation of a selection bias transformation function, those related to the GIDAS data, TBM model limitations, and others.

When it comes to the creation of a transfer function that can be applied to crashes generated by, for example, the TBM, there are three primary limitations. The first is that we do not know the shape of the complete set of PDOs (across all severities; the Folksam data we used have an inclusion criterion based on repair costs). In this work we assumed that the distribution shape exponentially decreased with delta-v. However, it may instead be, for example, a gamma distribution. Optimally, future work would acquire data on the relationship between delta-v and repair costs in order to determine the distribution's correct shape. (In addition, the manual adding of data can be automatized, although it is not likely to improve the model or model fitting substantially.) Second, the Folksam data used here include all kinds of frontal crashes. The PDO distribution is likely to be different if only rear-end crashes are included (given the GIDAS inclusion criteria used in this study). However, mainly the distribution's shape is used to create our transfer function (Eq. 2); we argue that it is not unreasonable to assume that the shape will be similar across at least many scenarios. The third and final main limitation related to the Folksam data is that we only have data on the injuries on the individual level, not on a per-crash level. This lack adds uncertainty to the estimates or the absolute values of the PDO distribution. Again, the fact that we primarily use the shape of the delta-v distribution should mitigate the impact of this limitation on the parameter fitting of the transfer function (Eq. 2).

There are two main limitations related to the GIDAS data used in this study. One is that we used a limited number of GIDAS crashes for validation. Having more cases would make the validation assertions firmer (and getting more out of the AEB assessment comparison). Another limitation, inherent to the GIDAS data (and all reconstructed pre-crash kinematics), is that the PCM data are just reconstructions, with assumptions about the pre-crash behaviors (although they are the best possible assumptions, given the available data; Hautzinger et al., 2005; Otte, 2003). Deceleration profiles and speeds are best estimates. This means that what

we really validate against in a paper such as this is the representation of the original crashes based on the assumptions in the reconstructions – it is not measured data. Appendix F provides further details on the GIDAS data in relation to crash-causation factors.

As for the TBM model, we acknowledge that it will not create all types of rear-end road crashes. That is, the causes of every crash are to some extent unique, and our model does not include more than a fraction of all possible causes of crashes. However, we argue that the TBM is likely to generate crashes representing the vast majority of rear-end crashes on highways. Although it is possible to develop crash-causation sub-models that represent even more crashes, the contribution to the overall pool of generated crashes from each added sub-model is likely to be small. Notably, though, the No-response sub-model should be further investigated. We used 10% No-response drivers due to sleepiness. Not only should the percentage used be anchored more firmly in literature, but there are also several other factors (in addition to off-road glances and sleepiness) that may result in No-response crashes. See Appendix F for more discussion on that topic.

There are certainly several areas where more crash-causation model research is clearly needed. Specifically, human behavior-related crash-causation models are needed for ADS (e.g., for take-over-requests) and ADAS, as trust in the systems increases and expectation mismatches become more common. Mismatch studies such as Victor et al. (2018) are important. The Victor et al. (2018) study found that approximately 30% of the drivers participating in the study crashed into objects in front of them, even when they had their eyes on the road; the drivers expected the vehicle system to avoid the crash automatically. However, it is not obvious to computationally model trust and expectations. More research is needed to pursue such modeling.

Further, our crash-causation model only covers rear-end car-to-car crashes. Much more work is needed to create and validate crash-causation models for other scenarios, such as car-to-vulnerable road users (e.g., cyclists and pedestrians). Also, inferential statistics have not been used in this study. A primary reason is that it is very difficult to test on distribution being the same, especially when the number of data points is not so large (i.e., here the GIDAS data). The distribution summary statistics in Appendix E provide may provide some insights, but we decided to focus on distribution visualizations and means. Finally, one limitation of the TBM relates to the No-reaction model: different from the other three sub-model, the No-reaction sub-model cannot easily be integrated in simulation of continuous driving (i.e., not only short-duration events), such as in traffic simulations.

## **5 Conclusions**

This work set out to validate a theory-based, rear-end crash-causation model (TBM), consisting of four sub-models, for scenario generation. Although the shape of the delta-v distribution of the generated crashes turned out to be similar to that of the GIDAS data, the former slightly underestimates the delta-v—with a distribution shifted towards lower-severity

crashes. In terms of mean delta-v, it was only marginally closer to the GIDAS mean than a substantially simpler model (BLOM, the brake-light onset-based model). However, the BLOM is not defined for approximately 37% of the original crashes (when the lead vehicle does not brake or is standing still during the entire event). Further, recent literature does not support brake-light onset followed by a reaction time as a model for driver responses in rear-end crashes, so it may only be by chance that the outcome of the simple model was relatively good. We argue that using TBM or similar crash-causation-theory based methods is more likely to capture both benefits and drawbacks of the technology under assessment, even if the resulting distribution slightly underestimates the delta-v.

Results from our sensitivity analysis showed that TBM was only marginally sensitive to the choice between two off-road glance distributions and the variation of two model parameters ( $\tau^{-1}$  and reaction time), indicating that the TBM is a relatively robust crash-causation model. While model robustness may be desirable, the validation will never be better than the underlying data, where selection bias is a genuine concern.

Although selection bias in crash databases is a common research topic, no work on selection bias related to the validation of virtual scenario generation appears to exist. The proposed method to compensate for the GIDAS (or other crash database) selection bias in the validation (by transforming the generated scenarios using models based on insurance data) seems to work reasonably well. Further, the selection bias transfer function seems to be relatively insensitive to the proportion of property-damage-only (PDO) crashes in real traffic. Note, however, that, a thorough validation of this method is difficult and will require more work. Specifically, more research on the design and validation of selection bias transforms for scenario generation is needed to: a) determine the shape of the full PDO distribution in the real world, b) extend it to and test it on different scenario categories (e.g., car-pedestrian interactions and car-car interactions at intersections), and c) validate the method itself (making sure that the validation method itself is accurate and robust).

The results show that delta-v distributions from different source data should not be compared without considering any possible selection bias in the data set(s). Clearly, the validation of scenario generation depends on being able to compare comparable data. There are also indications (although not as strong) that merely performing a validation of the injury risk (i.e., applying an injury risk function to both the validation data and the generated data) without addressing selection bias may not be advisable, either. Doing so is likely to substantially underestimate the injury risk.

This work demonstrates that, in order to validate scenario generation for virtual safety assessment, there is a clear need to understand the details of scenario generation, as well as of the validation dataset used—especially with respect to possible selection bias in the validation dataset. Research on methods for validating scenario generation for virtual assessment is rare; much more work is needed for virtual simulation to become the tool we

all want it to be, providing accurate estimates of safety benefits across all levels of crash severity.

### **Sponsor statement**

The findings and conclusions of this paper are those of the author(s) and do not necessarily represent the views of the SHRP2, the Transportation Research Board, or the National Academies.

### **Acknowledgements**

We want to thank the sponsors of this work, which include the QUARIS project, funded by the FFI program; and the V4SAFETY project, funded by the European Commission under grant number 101075068. We also want to thank Sava Iancovici for supporting on data extraction, Xiaomi Yang for supporting in the simulation implementation. Also Ulrich Sander, Carol Flannagan, and Linda Boyle deserve our gratitude for valuable discussions on part of this work. We also want to thank Anders Kullgren at Folksam, who made the insurance data available for this analysis. The SHRP2 data used in this study has the identifier DOI SHRP2-DUL-16-172 and was made available to us by the Virginia Tech Transportation Institute (VTTI) under a Data License Agreement.

### **References**

- Aust, M. L., Engström, J., & Viström, M. (2013). Effects of forward collision warning and repeated event exposure on emergency braking. *Transportation Research Part F: Traffic Psychology and Behaviour*, 18, 34-46. doi:<https://doi.org/10.1016/j.trf.2012.12.010>
- Benmimoun, M., Pütz, A., Zlocki, A., & Eckstein, L. (2013, 2013//). *euroFOT: Field Operational Test and Impact Assessment of Advanced Driver Assistance Systems: Final Results*. Paper presented at the Proceedings of the FISITA 2012 World Automotive Congress, Berlin, Heidelberg.
- Bjorvatn, A., Page, Y., Fahrenkrog, F., Weber, H., Aittoniemi, E., Heum, P., . . . Torrao, G. (2021). *Impact evaluation results (Deliverable D7.4 in the L3pilot project)* Retrieved from [https://l3pilot.eu/fileadmin/user\\_upload/Downloads/Deliverables/Update\\_14102021/L3Pilot-SP7-D7.4-Impact\\_Evaluation\\_Results-v1.0-for\\_website.pdf](https://l3pilot.eu/fileadmin/user_upload/Downloads/Deliverables/Update_14102021/L3Pilot-SP7-D7.4-Impact_Evaluation_Results-v1.0-for_website.pdf)
- Blatt, A., Pierowicz, J. A., Flanigan, M., Lin, P.-S., Kourtellis, A., Lee, C., . . . Hoover, M. (2015). *SHRP2 safety research - Naturalistic driving study: Field data collection (S2-S07-RW-1)*. Retrieved from Washington, DC: <http://www.trb.org/Main/Blurbs/170888.aspx>
- Bärgman, J., Boda, C.-N., & Dozza, M. (2017). Counterfactual simulations applied to SHRP2 crashes: The effect of driver behavior models on safety benefit estimations of intelligent safety systems. *Accident Analysis & Prevention*, 102, 165-180. doi:<https://doi.org/10.1016/j.aap.2017.03.003>
- Bärgman, J., Lisovskaja, V., Victor, T., Flannagan, C., & Dozza, M. (2015). How does glance behavior influence crash and injury risk? A 'what-if' counterfactual simulation using crashes and near-

- crashes from SHRP2. *Transportation Research Part F: Traffic Psychology and Behaviour*, 35, 152-169. doi:10.1016/j.trf.2015.10.011
- Bärgman, J., & Victor, T. (2019). Holistic assessment of driver assistance systems: how can systems be assessed with respect to how they impact glance behaviour and collision avoidance? *IET Intelligent Transport Systems*. Retrieved from <https://digital-library.theiet.org/content/journals/10.1049/iet-its.2018.5550>
- Bärgman, J., & Victor, T. (2020). Holistic assessment of driver assistance systems: how can systems be assessed with respect to how they impact glance behaviour and collision avoidance? *IET Intelligent Transport Systems*, 14(9), 1058-1067. Retrieved from <https://digital-library.theiet.org/content/journals/10.1049/iet-its.2018.5550>
- Ding, W., Xu, C., Arief, M., Lin, H., Li, B., & Zhao, D. (2023). A Survey on Safety-Critical Driving Scenario Generation—A Methodological Perspective. *IEEE Transactions on Intelligent Transportation Systems*, 1-18. doi:10.1109/TITS.2023.3259322
- Fajen, B. R. (2005). The scaling of information to action in visually guided braking. *J Exp Psychol Hum Percept Perform*, 31(5), 1107-1123. doi:10.1037/0096-1523.31.5.1107
- Fries, A., Fahrenkrog, F., Donauer, K., Mai, M., & Raisch, F. (2022). *Driver Behavior Model for the Safety Assessment of Automated Driving*.
- Gibbs, A., & Su., F. (2002). On choosing and bounding probability metrics. *Int. Statistical Review*, 70(3), 419–435.
- Green, M. (2000). "How long does it take to stop?" Methodological analysis of driver perception-brake times. *Transportation Human Factors*, 2(3), 195-216. doi:10.1207/STHF0203\_1
- Hautzinger, H., Pfeiffer, M., & Schmidt, J. (2005). *Expansion of GIDAS sample data to the regional level: statistical methodology and practical experiences*. Paper presented at the 1st International Conference on ESAR "Expert Symposium on Accident Research.
- He, D., & Donmez, B. (2022). The Influence of Visual-Manual Distractions on Anticipatory Driving. *Human Factors*, 64(2), 401-417. doi:10.1177/0018720820938893
- Helmer, T., Wang, L., Kompass, K., & Kates, R. (2015). *Safety Performance Assessment of Assisted and Automated Driving by Virtual Experiments: Stochastic Microscopic Traffic Simulation as Knowledge Synthesis*. Paper presented at the IEEE 18th International Conference on Intelligent Transportation Systems, Las Palmas.
- Hickman, J. S., Hanowski, R. J., & Bocanegra, J. (2010). *Distraction in commercial trucks and buses: Assessing prevalence and risk in conjunction with crashes and near-crashes*. Retrieved from Washington, DC: <http://ntl.bts.gov/lib/51000/51200/51287/Distraction-in-Commercial-Trucks-and-Buses-report.pdf>
- Horne, J., & Reyner, L. (1999). Vehicle Accidents Related to Sleep: A Review. *Occupational and Environmental Medicine*, 56(5), 289-294. Retrieved from <http://www.jstor.org/stable/27731108>
- Isaksson-Hellman, I., & Norin, H. (2005). How thirty years of focused safety development has influenced injury outcome in volvo cars. *Annu Proc Assoc Adv Automot Med*, 49, 63-77.
- Kiefer, R., Salinger, J., & Ference, J. J. (2005). Status of NHTSA's rear-end crash prevention research program. In *International Technical Conference on the Enhanced Safety of Vehicles*. Washington D.C.
- Klauer, S. G., Guo, F., Simons-Morton, B. G., Ouimet, M. C., Lee, S. E., & Dingus, T. A. (2014). Distracted driving and risk of road crashes among novice and experienced drivers. *New England Journal of Medicine*, 370(1), 54-59. doi:10.1056/NEJMsa1204142

- Knabe, E. (2023). Environment Simulator Minimalistic (esmini). Retrieved from <https://github.com/esmini/esmini>
- Knipling, R. R., Hendricks, D. L., Koziol, J. S., C., A. J., Tijerina, L., & Wilson, C. (1992). *A front-end analysis of rear-end crashes*. Paper presented at the IVHS America Second Annual Meeting, Newport Reach, California.
- Knipling, R. R., & Wang, J.-S. (1994). *Crashes and Fatalities Related to Driver Drowsiness/Fatigue*. Retrieved from file:///C:/Users/bargman/Downloads/dot\_2936\_DS1.pdf
- Kolmogorov, A. (1992). On the Empirical Determination of a Distribution Function. In S. Kotz, Johnson, N.L. (Ed.), *Breakthroughs in Statistics. Springer Series in Statistics*. New York, NY. : Springer.
- Kullback, S., & Leibler, R. (1951). On information and sufficiency. *Ann Math Stat* 22, 79–86.
- Kullgren, A. (2008). *Dose-response models and EDR data for assessment of injury risk and effectiveness of safety systems*. Paper presented at the 2008 International Research Council on the Biomechanics of Injury (IRCOBI), Bern, Schweiz.
- Kusano, K. D., & Gabler, H. C. (2012). Safety benefits of forward collision warning, brake assist, and autonomous braking systems in rear-end collisions. *IEEE Transactions on Intelligent Transportation Systems*, 13(4), 1546-1555. doi:10.1109/TITS.2012.2191542
- Lee, J. Y., Lee, J. D., Bärgrman, J., Lee, J., & Reimer, B. (2018). How safe is tuning a radio?: using the radio tuning task as a benchmark for distracted driving. *Accident Analysis & Prevention*, 110(Supplement C), 29-37. doi:<https://doi.org/10.1016/j.aap.2017.10.009>
- Leledakis, A., Lindman, M., Östh, J., Wågström, L., Davidsson, J., & Jakobsson, L. (2021). A method for predicting crash configurations using counterfactual simulations and real-world data. *Accident Analysis & Prevention*, 150, 105932. doi:<https://doi.org/10.1016/j.aap.2020.105932>
- Markkula, G., Engström, J., Lodin, J., Bärgrman, J., & Victor, T. (2016). A farewell to brake reaction times? Kinematics-dependent brake response in naturalistic rear-end emergencies. *Accident Analysis & Prevention*, 95, Part A, 209-226. doi:10.1016/j.aap.2016.07.007
- Miller, A., van Ratingen, M., Williams, A., Schram, R., Brasseur, M., Kolke, R., . . . Castaing, P. (2014). *2020 roadmap - european new car assessment programme (euroNCAP)*. Retrieved from
- Otte, D., Krettek, C., Brunner, H., & Zwipp, H. (2003). *Scientific Approach and Methodology of a New In-Depth- Investigation Study in Germany so called GIDAS*. Paper presented at the The 18th International Technical Conference on the Enhanced Safety of Vehicles (ESV).
- Schubert, A., Erbsmehl, C., & Hannawald, L. (2013). *Standardized pre-crash scenarios in digital format on the basis of the VUFO simulation input data from GIDAS*. Paper presented at the 5th International Conference on Expert Symposium on Accident Research (ESAR).
- Svärd, M., Bärgrman, J., & Victor, T. (2021). Detection and response to critical lead vehicle deceleration events with peripheral vision: Glance response times are independent of visual eccentricity. *Accident Analysis & Prevention*, 150, 105853. doi:<https://doi.org/10.1016/j.aap.2020.105853>
- US-DOT. (1998). *Summary report: Effects of a Towaway Reporting Threshold on Crash Analysis Result*. Retrieved from McLean, Virginia:
- van Lint, J. W. C., & Calvert, S. C. (2018). A generic multi-level framework for microscopic traffic simulation—Theory and an example case in modelling driver distraction. *Transportation Research Part B: Methodological*, 117, 63-86. doi:<https://doi.org/10.1016/j.trb.2018.08.009>

- Victor, T., Dozza, M., Bärghman, J., Boda, C.-N., Engström, J., Flannagan, C., . . . Markkula, G. (2015). *Analysis of naturalistic driving study data: SAFER glances, driver inattention, and crash risk (S2-S08A-RW-1)*. Retrieved from Washington, D.C.:  
[http://onlinepubs.trb.org/onlinepubs/shrp2/SHRP2\\_S2-S08A-RW-1.pdf](http://onlinepubs.trb.org/onlinepubs/shrp2/SHRP2_S2-S08A-RW-1.pdf)
- Victor, T., Tivesten, E., Gustavsson, P., Johansson, J., Sangberg, F., & Ljung Aust, M. (2018). Automation Expectation Mismatch: Incorrect Prediction Despite Eyes on Threat and Hands on Wheel. *Human Factors*, 60(8), 1095-1116. doi:10.1177/0018720818788164
- VTTI. (2015). *SHRP2 researcher dictionary for video reduction data - version 3.4*. Retrieved from Blacksburg, VA:
- Wang, J.-S. (2022). *MAIS(05/08) Injury Probability Curves as Functions of Delta V*. Retrieved from Wimmer, P. O. d. C., Olaf;Weber, Hendrik;Chajmowicz, Henri;Wagner, Michael;Lorente Mallada, Jorge;Fahrenkrog, Felix;Denk, Florian. (2023). *Harmonized Approaches for Baseline Creation in Prospective Safety Performance Assessment of Driving Automation Systems*. Paper presented at the The 27th Enhanced Safety of Vehicles (ESV) Conference, Yokohama, Japan.
- Ydenius, A., Stigson, H., Kullgren, A., & Sunnevång, C. (2013). *Accuracy of Folksam Electronic Crash Recorder (ECR) In Frontal and Side Impact Crashes*. Paper presented at the 23rd International Technical Conference on the Enhanced Safety of Vehicles (ESV), Seoul, South Korea.

## **Appendix A – The rationale for the assumption of 70% PDO for rear-end in real-traffic**

In Knipling et al. (1992) it is stated that in the year 1990 in the US there were 1.5 million police-reported rear-end crashes on roadways with roughly 800,000 associated injuries and 2,078 associated fatalities. It is also approximated, depending on methodology used, that there is an additional unreported number of PDO rear-end crashes between 1.3 million and 1.75 million. This gives a range of a total of 2.8 million to 3.25 million rear-end crashes and 800,000 of these being injuries, the rest PDO crashes. Expressed in percentage the PDO crashes is then approximately 71% to 75% . In this paper we use the conservative number of 70%.

## Appendix B - Estimation of delta-v

The impact speed for the following vehicle from each simulation is estimated by assuming a one-dimensional inelastic collision between the following- and lead vehicle host. Due to the nature of car crashes in general (kinetic energy is not conserved), as well as the specific conflict situation studied (rear-end crashes), this estimation is shown to be reasonable, as seen in Appendix D.

Figure B1 shows a diagram of the lead- and the following vehicle in an inelastic collision. The impact speed for the following vehicle from each simulation is then estimated as the change in speed for the following vehicle before and after the collision.

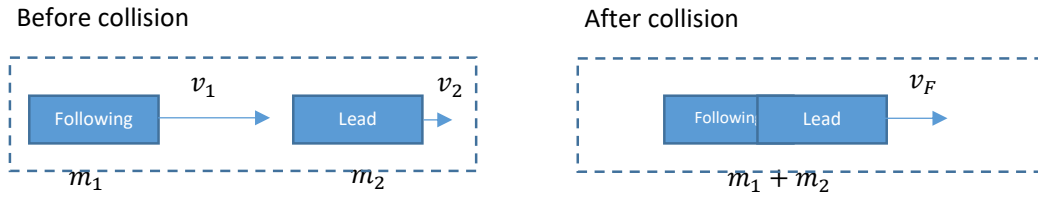


Figure B1: Diagram of involved actors in an inelastic collision

Conservation of momentum in the system before and after the collision yields Equation 1. The speed reduction for the following vehicle,  $\Delta v_1$ , is according to Equation B2.

$$m_1 v_1 + m_2 v_2 = (m_1 + m_2) v_F \quad (\text{B1})$$

$$\Delta v_1 = v_1 - v_F \quad (\text{B2})$$

Solving Equation B1 for  $v_F$  and substituting into Equation B2 yields:

$$\Delta v_1 = v_1 - \frac{m_1 v_1 + m_2 v_2}{m_1 + m_2} = \frac{m_2 (v_1 - v_2)}{(m_1 + m_2)} \quad (\text{B3})$$

In practice,  $v_1$  and  $v_2$  are taken from the simulation output at the point in time where the following- and the lead vehicle first overlap, and  $m_1$  and  $m_2$  are taken from the corresponding crashes in GIDAS. Note, as seen in Equation 3, if the involved actors have the same mass, then

$\Delta v_1$  can be estimated as simply  $\frac{v_1 - v_2}{2}$ . This estimation was also studied in Appendix D, which can be useful when one lacks information about the relative masses of the involved actors.

## Appendix C – The overshoot distribution

The part of the glance that extends beyond the  $\tau^{-1}$  threshold is called the overshoot. If one assumes that the probability that any driver starting to look off-road is independent of the critical event initiation (e.g., that a lead vehicle brakes hard), it is possible to create what is called an overshoot distribution that is placed at  $\tau^{-1}=0.2s^{-1}$ . To exemplify, consider the driver's distribution of off-road glances while driving shown in Figure 1 and imagine an off-road glance duration of 0.3s. This glance can be placed so that all of it overshoots  $\tau^{-1}=0.2s^{-1}$ , or 0.2s overshoots, or 0.1s overshoots. With the assumption that there is a uniform probability that the critical event will occur at any time during the 0.3s, the three glances have an equal probability of occurring (i.e., 1/3). For an off-road glance of 0.4s, overshoots of 0.1, 0.2, and 0.3s, and even 0.4s can occur. Now each of the four durations has a probability of 1/4 of occurring. For a 0.2s glance, only 0.1 and 0.2 can occur (with a probability of 1/2), and for a 0.1 glance only 0.1s can occur (with a probability of 1). This means that in terms of the overshoots of an entire off-road glance distribution, the probability of a short glance overshoot is much higher than the probability of a long glance overshoot (consider the sum of probabilities for 0.1s compared to 0.4s in the section above). There is actually a statistical transformation that can be performed (instead of running all these simulations) to convert a probability density function of off-road glance durations into an overshoot distribution. See Extra Material for the code of the transformation. The benefit of this transformation is that it can be placed at the overshoot anchor, which here is  $\tau^{-1}=0.2s^{-1}$ . This action reduces the dimensionality by one. That is, simulations are no longer needed for all combinations of possible overshoots. For example, instead of having to run  $4+3+2+1=10$  simulations for the 0.4, 0.3, 0.2., and 0.1s off-road glance durations, only four simulations are needed (one for each glance duration).

## Appendix D: Validation of delta-v

### Estimation of change in velocity during the collision, $\Delta v$

The goodness of the estimation of  $\Delta v$  by the chosen method was assessed by applying the method to the PCM-data from GIDAS, in the same way as described in the method. For the PCM data we used the last data point, which corresponds to the index of collision, and applied the same equations. This process was performed for the 103 cases which fit the selection criteria. Figure D1 shows the estimated impact speeds vs the reported impact speeds in GIDAS; the estimate was shown to be very good for most of the cases. Figure D1 also shows that if one does not consider the relative masses of the actors, this estimation is less accurate.

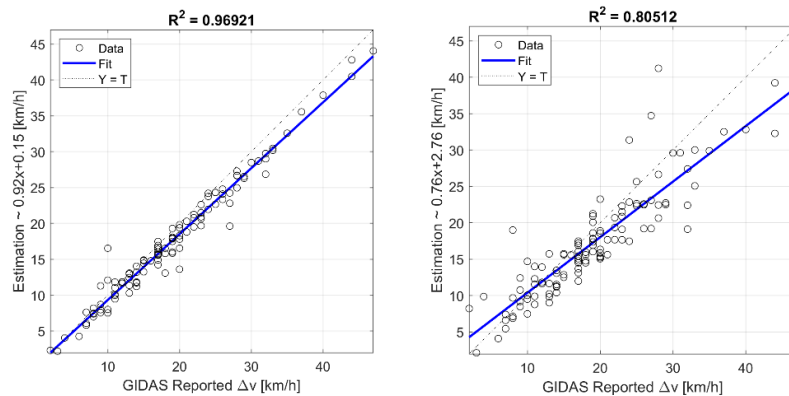
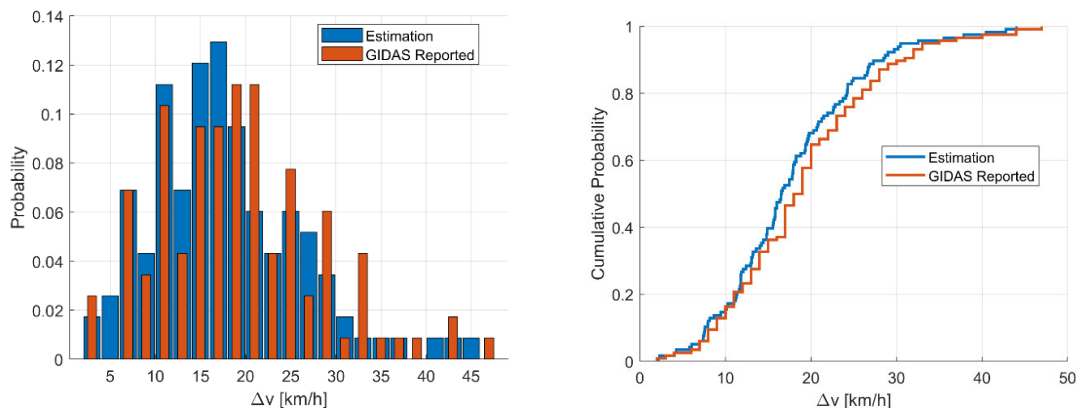


Figure D1: Linear regressions of the relation between the  $\Delta v$  reported in GIDAS and the estimation used in the paper (left) and a simpler estimation that does not take the relative masses into account (right).

Since the chosen method still has some errors, the effect of these errors on the impact speed distribution was also analyzed—by comparing the impact distributions in the GIDAS original cases with the distribution of the estimated impact speed, using the selected method. Figure D2 show the magnitude of the effect of the impact speed estimation on the impact speed distribution.



*Figure D2: Impact speed distribution difference between GIDAS original and the estimation (left panel), and the corresponding cumulative density function*

## Appendix E – Distribution summary statistics

For an enthused reader, Table E1 shows summary statistics used to compare the different models in this work. Below each of the metrics is described in turn.

- Absolute difference from mean – the difference in mean of the compared distributions
- Mean absolute difference – the mean of the difference of each individual impact speed bin between the compared distributions, without taking the probability of each bin into account.
- Weighted mean absolute difference – the mean of the difference of each individual impact speed bin probability weighted using the probabilities of each respective bin.
- Maximum absolute difference – the maximum difference between two bins between the two compared distributions.
- Total variation distance – the normalized L1 distance between two distributions, indicating how much the distributions overlap or diverge:  $D_{TV}(p, q) = \frac{1}{2} \sum_{i=1}^N |p(x_i) - q(x_i)|$ , where N denotes the number of distribution bins,  $p(x_i)$  is the weight of the i:th bin in the generated output distribution and  $q(x_i)$  is the weight of the corresponding bin in the distribution used for comparison (in our case, the GIDAS data). (Gibbs & Su., 2002; Kullback & Leibler, 1951)
- KL-divergence – the difference in information (entropy) between two distributions, calculated as:  $D_{KL}(p, q) = \sum_{i=1}^N p(x_i) \log \frac{p(x_i)}{q(x_i)}$ . Since the KL-divergence cannot handle non-zero bin weights, half a count was added to each distribution bin and the resulting corrected distributions were then re-normalized. (Gibbs & Su., 2002)
- KS test statistic – the maximum vertical distance between the empirical CDF:s of the compared distributions:  $D_{KS}(p, q) = \sup_{i \in \{1, \dots, N\}^c} |p(x_i) - q(x_i)|$  (Kolmogorov, 1992)

Note that for most of the metrics several weighting steps are needed (i.e., case/propensity weighting, selection bias transform, and the probability that each case would occur, given the off-road glance and maximum deceleration probability). These steps are described in each respective method description.

Table E1: Distribution-comparison statistics where different models are compared with the original delta-V distribution. See section 2.8.1 for details about the metrics.

Metric	TBM transformed ( $\tau^{-1}=0.2s^{-1}$ ; RT=0.5s; Kungälv glances)	BLOM	TBM transformed ( $\tau^{-1}= 0.3s^{-1}$ )	TBM transformed (RT= 0.8s)	TBM transformed (SHRP2 glances)	TBM not transformed
Mean (GIDAS original=Xkm/h)	15.53	21.63	15.88	15.00	15.69	10.31
Absolute difference from (full) mean	2.98	3.12	2.63	3.51	2.82	8.20
Mean (full) absolute difference	0.00798	0.00782	0.00714	0.00713	0.00759	0.0163
Weighted (full) mean absolute difference	0.0275	0.0187	0.0243	0.0224	0.0261	0.0368
Max absolute difference	0.0788	0.0610	0.0812	0.0830	0.0798	0.122
Total variation distance	0.239	0.235	0.214	0.214	0.228	0.488
KL-divergence	0.337	0.276	0.313	0.345	0.330	0.953
KS-distance	0.204	0.162	0.186	0.199	0.174	0.487

## **Appendix F – Details limitation related to other crash-causation factors**

The high-level statistics of factors, not directly related to the GIDAS PCM, were studied from the included cases in the GIDAS database in order to consider whether the developed model would be expected to cover them. The two main categories, ‘environment’ and ‘driver’, are discussed below. Just because these factors are coded in GIDAS does not mean they are always the main cause of the crash, but they are likely to be contributing factors. One must also remember that the lack of reports on these factors does not necessarily mean that they are not important in reality.

Parameters identified in GIDAS as environment-related factors include rain and snow and their effect on braking performance, as well as rain, snow, fog, and darkness and their effect on glance behavior and visibility. The factors affecting braking performance is in this work partially captured by the use of a distribution of maximum driver decelerations. However, the TBM does not, for now, consider visibility factors.

Driver-related factors include, for example, medical conditions such as heart attack, seizures, cramps, and fatigue. The 10% added to the model to represent sleepy drivers will cover these factors to some extent, but further investigations should be made into their prevalence. Note that if it is found that these factors play a larger role (than what is captured in the 10% no-reaction crashes) it is possible to adjust the percentage no-reaction crashes. Further, in-depth crash investigations have shown that factors such as the view of the target being obstructed by the sun visor, glare from the sun, or other traffic participants also may contribute to crashes. However, since the model assumes perfect visibility when there is no off-road glance, these factors are not explicitly captured in the TBM. However, also if future research indicate that such factors are a substantial part of crashes, the proportion of no-reaction crashes may be adjusted also to cover these factors.

There are also underlying driver parameters such as age, general medical conditions, and medications—as well as the current state of the driver (including the use of alcohol or other drugs). The variability of the input data (glance behavior data and maximum deceleration, as well as other parts of the TBM) likely capture some of these, but far from all. Future studies may go into detail on these factors to investigate if it is possible (and there is a need) to consider them in the crash-causation models (e.g., introducing minor changes in the response model).

Further driver-related factors are related to the driver’s ability to judge the absolute and relative speeds and distances in traffic, as well as mismatches between driver expectations and what actually happen on the road (e.g., if a lead-vehicle driver is suddenly aborting a overtaking). Also these factors are partially captured in the glance behavior and maximum deceleration data, but further research is needed, especially on how to model expectation mismatches (see [ref Giulio], for one example of expectation mismatch in an ADS setting).